ABSTRACT

Quantitative Assesment of Myocardial Oxygen Supply and Demand Using a Dynamic Model of the Cardiovascular System

by

Badrinath R. Puranic

A quantitative understanding of the changes in coronary, pulmonary and systemic hemodynamic variables and their effect on myocardial supply and demand is important to the better management of anesthetic care of patients with impaired cardiac function. Animal studies have identified those hemodynamic factors that play an important role in determining the balance between oxygen supply and demand for the myocardium. These include myocardial contractility, left ventricular end-diastolic volume, systemic arterial pressure, systemic vascular resistance, and heart rate. The interactions of these factors are complex and their combined effects on myocardial oxygen supply and demand are difficult to predict a priori.

The objective of this work was to construct a mathematical model of the cardiovascular system which will allow us to simulate the effects of changes in one or more of those hemodynamic parameters on myocardial supply and demand. The model used is a combination of several models which have been reported in the literature, along with our own modifications. The important feature of the model is that it is dynamic in nature and thus it is helpful in real time analysis. The model is also useful to conceptualize the problem and test relationships, helping researchers frame hypothesis and design experiments.

QUANTITATIVE ASSESSMENT OF
MYOCARDIAL OXYGEN SUPPLY AND DEMAND USING
A DYNAMIC MODEL OF THE CARDIOVASCULAR SYSTEM

by
Badrinath R. Puranic

A Thesis
Submitted to the Faculty of
New Jersey Institute of Technology
in Partial Fulfillment of the Requirements for the Degree of Master of Science
in Biomedical Engineering
October, 1992

APPROVAL PAGE

Quantitative Assessment of Myocardial Oxygen Supply and Demand Using a Dynamic Model of the Cardiovascular System

by

Badrinath R. Puranic

Dr. Yun Q. Shi, Thesis Adviser
Professor of Electrical and Computer Engineering
New Jersey Institute of Technology

Dr. Arthur B. Ritter, Thesis Adviser
Associate Professor of Physiology
University of Medicine and Dentistry of New Jersey

Dr. Alex Bekker, Committee Member
Resident in Anesthesiology
Columbia Presbyterian Medical Center

Dr. David Kristol, Committee Member
Professor of Chemistry and Director of Biomedical Engineering
New Jersey Institute of Technology

BIOGRAPHICAL SKETCH

Author: Badrinath R. Puranic

Degree: Master of Science in Biomedical Engineering.

Date: October, 1992

Date of Birth: March 28, 1967.

- Master of Science in Biomedical Engineering, New Jersey Institute of Technology, Newark, NJ, 1992

- Bachelor of Science in Electronics and Telecommunications Engineering, B. M. S. College of Engineering, Karnataka, India, 1990

Major: Biomedical Engineering

Presentations and Publications:

Puranic, Badrinath R., A. B. Ritter, A. Bekker, and D. Kristol. "A Model of Cardiovascular Function for Regulation of Anesthesia."Presented in Rhode Island, March 1992, at the IEEE Northeastern Bioengineering Conference, Rhode Island, USA. n. p., 1992.

Puranic, B. R., and Sanand P., "ISDN - Concepts and Issues." Presented in Bangalore, India, January 1989, at the IEEE Student Conference, India. n. p., 1989.

This thesis is dedicated to my family

ACKNOWLEDGEMENT

TABLE OF CONTENTS

Page

LIST OF TABLES

LIST OF FIGURES

ix

CHAPTER 1
INTRODUCTION

1.1 Introduction

Therapeutic management of critically ill patients requires a careful balance between oxygen delivery to various organs and oxygen consumption by the myocardium. Many studies have shown that improved oxygen delivery improves patient survival [24]. Since measurement of myocardial oxygen supply and demand is difficult, these variables must be estimated from other easily measurable hemodynamic parameters such as pressures, flows, etc. In that case, a computer model of the systemic circulation which can simulate the hemodynamic changes which occur in response to administration of various doses of different drugs will be helpful in predicting the changes in myocardial oxygen supply and demand associated with a given treatment modality. Such simulations could prove useful in the management of critically ill patients where there is little or no time to optimize treatment modalities.

1.2 Importance of Maximizing Body Oxygen Uptake and Balancing Oxygen Supply/Demand of the Heart

In health, oxygen consumption is a closely regulated phenomenon, oxygen being the critical electron acceptor in the generation of energy from metabolic fuel substrate. However, in conditions of altered metabolic states such as are seen in patients after injury or during severe sepsis, oxygen consumption increases, especially when these conditions are associated with an increase in body temperature. Conversely, in hypovolemic, ischemic, cardiogenic, or vasodilatory shock states, oxygen consumption decreases, falling below the

oxidative requirements of the various organ metabolic processes. The oxygen debt produced results in a severe metabolic acidosis. The concept of oxygen debt is illustrated in Figure 1 [25].

With reference to Figure 1, normal resting oxygen consumption in young men has been shown to average 140 mL/min per square meter of the body surface area, which is equivalent to approximately 3.5 mL/min per kilogram of body weight, or 250 mL/min in the 70 kg. textbook man [26]. The normal rate of MVO_2 is reduced by the restriction in tissue perfusion occuring in hypovolemic shock. This decrease in MVO_2 below the obligatory oxidative needs produces an oxygen deficit (oxygen debt) over time. If resuscitation occurs early in the process, before a critical level of ischemia has been reached, there is a rapid repayment of the oxygen debt., with an overshoot, in which the unmetabolized metabolic acids are oxidized with full recovery from the ischemic condition. If the oxygen debt remains unrepaid or is increased for a longer period of time, critical cellular injuries occur, with intracellular organelle disruption and death of the most vulnerable cells, leaving the individual with significant organ damage - primarily in the organs with high oxidative requirements: brain, liver, kidney, myocardium, and immunologic tissues. These cellular injuries induced by acute ischemia leads to later complications related to failures of organ function. The specific effects of these failures of cell and organ function are revealed clinically as an altered host defense, which predisposes to sepsis, or as a decompensating organ injury, as is seen in the post-ischemic brain syndrome. Finally, if the oxygen debt is unrepaid for a long enough period, the debt accumulates to a level at which sufficient lethal cell injury is present to prevent recovery, and death may
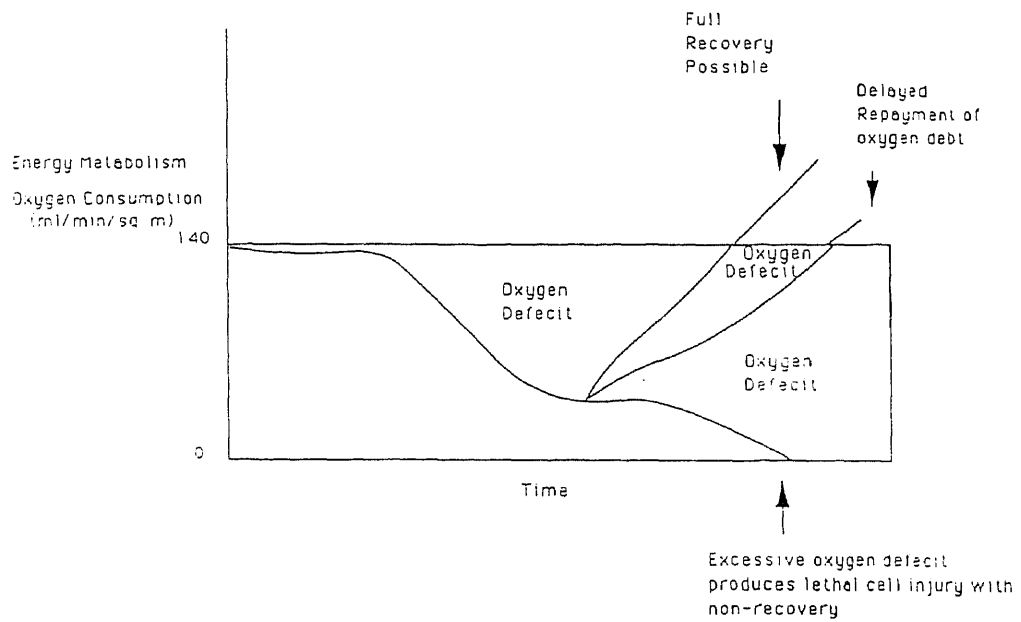
Figure 1 Diagrammatic Representation of the Accumulation and Repayment of Oxygen Debt

follow, often associated with the so-called multiple organ failure syndrome (MOFS) [25].

In patients with coronary artery disease, oxygen delivery to the heart is limited because of impaired coronary blood supply. Therefore, an important guideline for anesthesia, as well as any cardiovascular therapy, is the effect of myocardial demand. Routine monitoring of myocardial oxygen uptake (MVO$_2$) is not practical in patients, because measurement of MVO$_2$ requires considerable effort, including a coronary sinus catheter, analysis of arterial and coronary sinus blood samples, and measurements of myocardial blood flow. Therefore, clinical therapy often must be based on the estimation of myocardial oxygen demand from hemodynamic variables [11]. Computer modeling may prove very valuable in simulating various clinical situations and comparing alternative therapies.

1.3 Overview of a Few Cardiovascular Models -Advantages and Limitations

Drugs do not act on pressures, volumes, or flows within the circulation. They act directly or indirectly on the smooth muscle and cardiac muscle and, in a few cases, on noncontractile elements to alter, for example, heart rate or blood viscosity. Smooth muscle is distributed through the vascular system and at each point it influences the resistance to the flow of blood within the vessel. To describe this system, the concepts of parallel and series coupled sections of the vascular bed have been developed. The various organs are generally coupled in parallel while, within each organ, specialized sections coupled in series can be described. These ideas lead directly to the concept of compartments in the vascular system, each containing a finite volume of blood at a finite pressure separated from each other by resistances. It can be

seen clearly that the smaller number of compartments, the more easily the system is described. Hence a frequently used model [9, 10] involves four compartments - arterial, capillary, venous, and cardiopulmonary - as shown in Figure 2. Each compartment is considered to be separated by a section with smooth muscle that varies the compliance of the compartmental walls. Unfortunately, although it is the activity of the vessel smooth muscle that causes variations in flows, pressures, and volumes in the compartments, this smooth muscle activity cannot be measured independently except in some preparations in vitro. Thus we are forced to the circular argument of determining the resistances and compliances from the flows, pressures, and volumes.

When resistances or compliances in series or parallel are considered, the analogue of an electrical direct current circuit is often used. This analogue is particularly useful when resistance networks are considered. This analogue shows that pooling resistances between beds for arteriolar, postcapillary, and venous resistances, as was done in the single model in Figure 2, is invalid unless the capillary and venous pressures are identical in all organs. Thus the model in Figure 2 would predict that a drug that dilated arterioles in the kidney would have the same effect on cardiac output and arterial pressure as a drug that produced the same degree of vasodilation in the splanchnic bed. This conclusion is incorrect since vasodilation in the kidney raises renal venous pressure but causes little change in blood volume distribution since renal compliance is small. On the other hand, vasodilation in the splanchnic bed raises portal pressure and causes marked changes in blood volume distribution since splanchnic venous compliance is large. Therefore, a satisfactory model of the circulation requires separation of at least the major
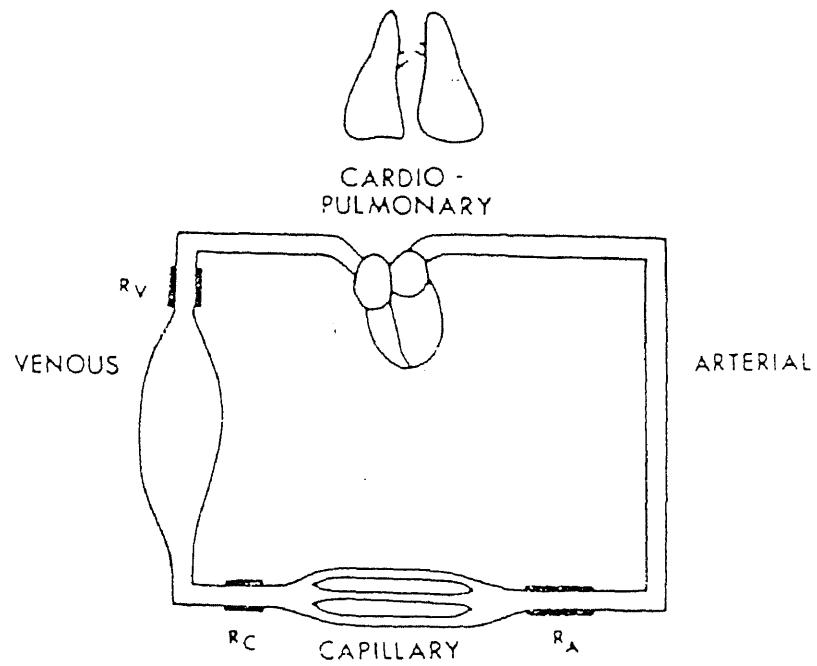
Figure 2 The Simple Four Compartment Model of the Circulation. R_A, R_C, and R_V are the Arteriolar, Postcapillary, and Venous Resistances Respectively

peripheral vascular beds, and pooled values for the series-coupled resistances cannot be used. Although the electrical analogue for circulatory resistances appears to be valid, it is inappropriate when used to model compliances. In a direct current electrical circuit, insertion of a capacitor in series causes current flow to stop, while in parallel current flow is unaltered after the capacitor is charged. Both situations clearly do not apply to the circulation. Even greater limitations in the model shown in Figure 2 arise in relation to the cardiopulmonary compartment. This is generally considered as a whole and right atrial pressure is related directly to cardiac output or stroke work. Hence the many intricate cardiovascular relationships in this compartment cannot be described. Thus there is need for a model that separates the major components of the peripheral vascular bed and that allows separation of the heart into four pumps separated by pulmonary, arterial, and venous compartments.

Schmid et Al [23] have studied hemodynamic determinants of myocardial oxygen supply and demand. They used a computer model which combines the time-varying elastance model of the left ventricle, the modified Windkessel model of the arterial system, and the left ventricular pressure-volume area prediction of oxygen demand. Their work represents an important step in understanding the role of hemodynamic determinants of myocardial oxygen supply and demand which are difficult to measure in real life. Due to the simplicity of their model, however, the results can only be used to predict gross changes in those variables which cause myocardial ischemia.

Guyton's work [9, 10] on system analysis for the cardiovascular system has a major contribution to circulatory physiology. Guyton's analysis of the circulation in the cardiovascular system is based on the concept of mean

circulatory filling pressure - the equilibrium pressure developed throughout the circulation when cardiac output is zero. Although the concept is sound, the circulation is never at rest; this mean circulatory filling pressure cannot be measured in man and although it can be estimated within a few seconds in dogs, smooth muscle activity has at least begun to change within these few seconds and repeated episodes of ventricular fibrillation cannot improve the state of the preparation. In addition, the precise equations used to describe the relationships were not discussed and the analysis was presented only as a flow chart. For these reasons, this system analysis has not had a great impact on the interpretation of mechanisms of drug effects on the circulation.

C. V Greenway [8] presents a new model of the circulation wherein he has adopted a set of equations from the work of Levy [13] on cardiac and vascular factors that determine systemic blood flow. There are three basic sets of equations that describe the equilibrium condition of the circulation namely - the resistance equations, the compliance equations, and the cardiac equations. Of particular interest are the cardiac equations developed by Greenway that relate the function of the heart to its preload and afterload. He has assumed the following relationship:

$$P_{ed} = P_{at} + k F_{at} \qquad (1)$$

where P_{ed} is end-diastolic ventricular pressure, P_{at} is mean atrial pressure, k is a constant, and F_{at} is an arbitrary measure of atrial contractility. This work falls short of validating acceptable values for k and F_{at}. Moreover Greenway has used only two values for the left ventricular contractility, E_{max} and E_{min}. But in reality, left ventricular contractility is a time-varying function as shown by extensive work on the contractile state of the left ventricle by H. Suga and K. Sagawa, and K. Sungawa and K. Sugawa [29, 33].

This work suggests that constant end-systolic pressure-volume relationship and ventricular curves relating stroke work or cardiac output to end diastolic volume or pressure can be obtained only if single values are used for E_{max} and E_{min}, while an analysis based on the contractility function curves did not give constant end-systolic pressure-volume relationships. Greenway has no explanation for this.

Mc Leod [16], has developed a model of the cardiovascular system which is referred to as the Physiological Benchmark Model - PHYSBE, using the TUTSIM simulation package. There is a major shortcoming in this model, where all the pressures, volumes, and flows reach zero after a short period of time (t = 50 sec). In a closed loop model these variables should never go to zero, instead they should reach a steady state with time and stay at their steady state values for the duration of the simulation.

1.4 Motivation and Objectives

Medical diagnosis and therapeutic monitoring for critical illness require adaptation of laboratory techniques to the bedside. These are immensely helped by the modification of physiological and biochemical data acquisition techniques to increase the number and accuracy of noninvasive variables that can be obtained from the patient.

The estimation of myocardial oxygen supply and demand from routine monitoring of patients is not practicable. Therefore, there is a need for estimating the myocardial oxygen supply and demand with noninvasive techniques in as simple a manner as possible. A dynamic model of the cardiovascular system which can predict myocardial oxygen supply and demand proves to be an useful tool with regards to the problem. The

simulation makes the model easy to use on a personal computer with minimal effort.

The energy requirements of the working heart have received much attention over the years. In the heart, unlike skeletal muscle, the conversion of chemical energy to mechanical work is highly dependent on oxidative reactions. An oxygen debt leads to a decline in ventricular performance. As a result the heart is considered to be an obligate aerobic organ. The interrelation between oxygen requirements and oxygen availability, synonymous with the concept of metabolic demand and supply, is fundamental to any consideration of the heart's capacity for work. A good model of the cardiovascular system is required in order to predict myocardial oxygen supply and demand with reasonable accuracy. On reviewing several models of the cardiovascular system, there is a need for a model which includes the important features of the cardiovascular system together with possible improvements.

CHAPTER 2
MODEL OF THE CARDIOVASCULAR SYSTEM

2.1 The Computer Model

To formulate a model of the cardiovascular system, the system has been divided into 18 components: the pulmonary system; consisting of the pulmonary arterial, capillary, and venous systems, left ventricle, aorta, large arteries, arterioles, systemic capillaries, venules, large veins, vena cava, and the right ventricle along with the coronary circulation, brain, kidneys, hepatic artery, liver, spleen and GI tract, and a skeletal muscle compartment. Each of these compartments is assumed to have a characteristic resistance and a compliance. Figure 3 shows a schematic of the circulatory system.

The basic resistance equation states that pressure drop between compartments is a function of the flow and the resistance to flow between the compartments. The basic equation which states its relationship, between any two compartments (e.g. 1 and 2) is:

$$P_1 - P_2 = Q * R \tag{2}$$

where P_1 and P_2 are the pressures in compartments 1 and 2 on either side of the resistance R and Q is the flow from compartment 1 to compartment 2. This well known equation is derived from Pouseilles's law and is analogous to Ohm's law. The resistance is primarily determined by the composite radius of the vessels, although changes in viscosity of the blood will also alter resistance. As discussed before, it is necessary to consider each vascular bed separately. Within each bed, the arteriolar, postcapillary, and venous
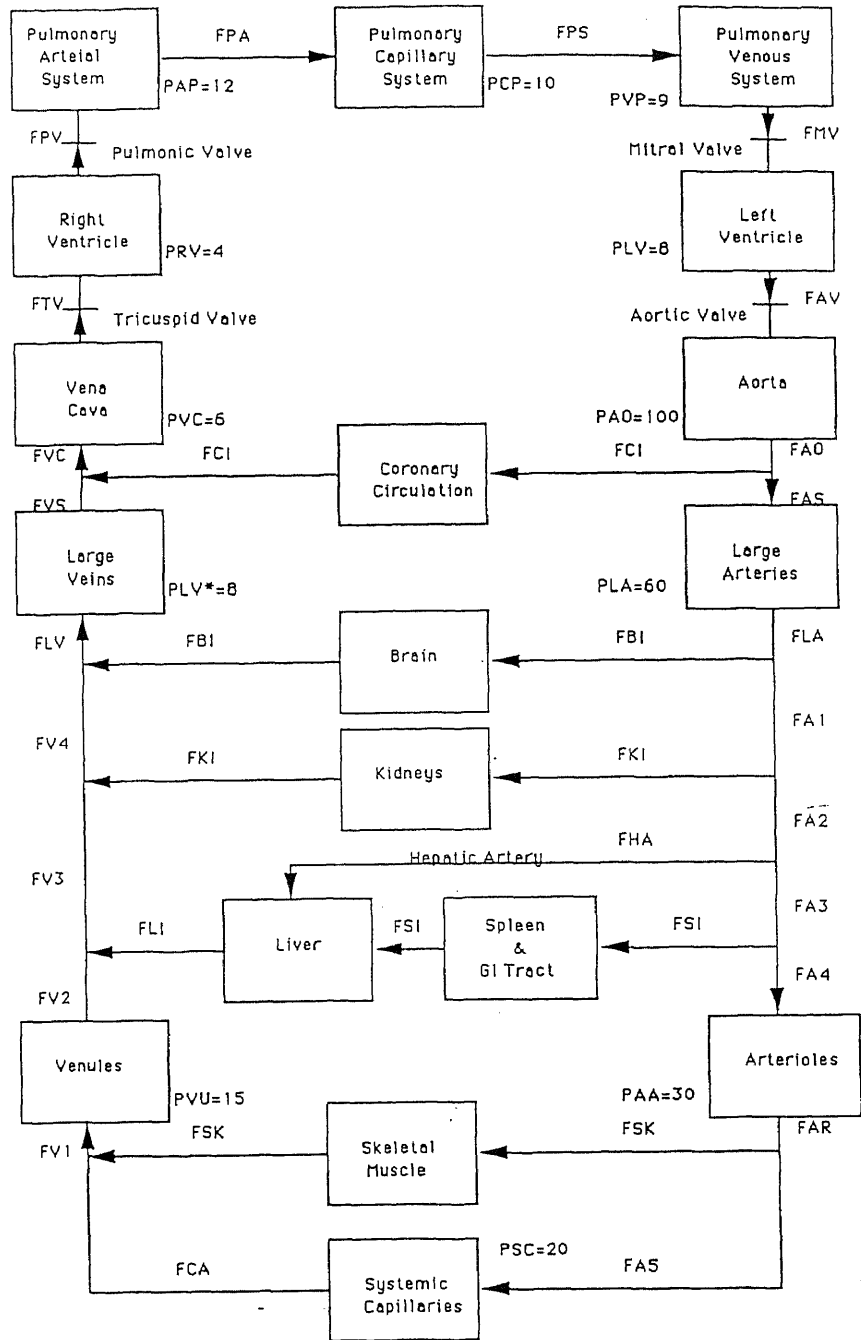
11

Figure 3 Schematic Diagram of The Systemic Circulation Showing The Series-Parallel Arrangement of Compartments Used in the Model

resistances are in series and can be added to obtain the total resistance in that bed. Thus these equations determine the pressures in all compartments of the circulation relative to the pressures in adjacent compartments. They do not determine the absolute transmural pressure in any compartment.. This is determined by the compliance equations. The above equations refer to a static circulatory system, i.e. the pressures are not varying with time. A dynamic system is realized if the pressures and flows vary with time and this is what is accomplished by our model:

$$(dP_1/dt) - (dP_2/dt) = (dQ/dt) * R \qquad (3)$$

where P, Q and R represent the same as above.

Within each compartment, transmural pressure is a function of the blood volume in the compartment and the compliance of its walls:

$$dP/dt = (1/C) * (dV/dt) \qquad (4)$$

where P is the transmural pressure, V is the volume, and C is compliance of a particular compartment This relation assumes a linear relation between volume and pressure, with the volume decreasing to zero when pressure is zero. Other models have assumed a finite volume of blood in the circulation at zero pressure. However, this volume cannot be measured accurately and it changes; therefore equations of this type will be very complex. In addition the shapes, slopes, and intercepts of pressure-volume curves obtained with currently available methods are so variable that it is not yet possible to formulate accurate equations. Therefore, equations as simple as possible were used in this analysis. When both the resistance and compliance equations for all the compartments are simultaneously satisfied, the pressures and volumes throughout the circulation are described.

To give an electrical analogy of the cardiovascular system, the left and the right ventricles are simulated by an electrical analog circuit consisting of a

series resistance and a time varying capacitor in parallel. One way valves representing atrioventricular, aortic, and pulmonic valves are used to direct flow into and out of the ventricles in an appropriate manner during each cardiac cycle. The aorta and the pulmonary artery are represented by a series arrangement of a conductor and a parallel capacitor. The large arteries, arterioles, venules, large veins, vena cava, skeletal muscle, and the systemic, coronary, pulmonary, and hepatic circulations are represented by series-parallel arrangements of resistors and capacitors as in the Windkessel model. In this model, electrical voltage is the analog of pressure, electrical charge represents blood volume, and electrical current represents blood flow. Electrical capacitance represents storage of blood volume and the reciprocal of compliance (capacitance) is the elastance of the vessels. The elastance of the heart was made to change periodically in accordance with a set of pre-chosen values. A similar concept of time-varying elastance or reciprocal compliance has often been used by modelers of the circulatory system in simulating the ventricular pump performance. This analysis has adopted the time-varying elastance concept from Suga and Sagawa's [29] work on Instantaneous pressure-volume relationships in the canine left ventricle. The following section gives a brief validation for the use of the time-varying elastance used in our model.

2.2 Time Varying Pressure-Volume Ratio

The mean E(t) curve and the standard deviation from a set of five to ten consecutive beats under each loading condition for each contractile state was calculated by the computer [29]. This output was recorded on an x-y plotter. The pressure-volume ratio curves obtained for a given contractile state were similar in contour and magnitude regardless of the drastic difference in the

loading conditions. The top of Figure 4 shows examples of computer produced mean $E(t)$ curves, one from isovolumic beats and the other from auxobaric beats. The bottom of the figure shows examples of the means of the mean $E(t)$ curves acquired under the different loading conditions and a constant contractile state in one heart. As the curves indicate, there was little difference between the isovolumic and auxobaric $E(t)$ curves at any time in systole. The diastolic phase of the curve in auxobaric contractions was situated slightly lower than that in isovolumic ones. Statistical analysis showed that the peak value of the pressure-volume ratio curve, E_{max}, was unaffected by the changes in loading condition (standard deviation of the mean E_{max} in a given preparation was 3-4%). Moreover, the time to E_{max}, from the onset of systole, T_{max}, was not affected by the changes in end-diastolic volume (standard deviation of the mean T_{max} in a given ventricle was about 6%). T_{max}, however, was slightly prolonged with the change of the contraction mode from isovolumic to auxobaric. These findings were common to both the control and the enhanced contractile state.

By contrast, inotropic interventions significantly affected the pressure-volume ratio curve. Two examples of the inotropic effects are shown in Figure 4. With the infusion of isoproterenol or norepinephrine, contractile state was markedly enhanced as reflected by a mean increase of 56% in peak isovolumic ventricular pressure. The mean increase in E_{max} for all nine hearts was 63%. Mean T_{max} was shortened by 10%. The statistical data for E_{max} and T_{max} are given in Table 1. Similar changes occured whether or not heart rate was kept constant by artificial pacing.
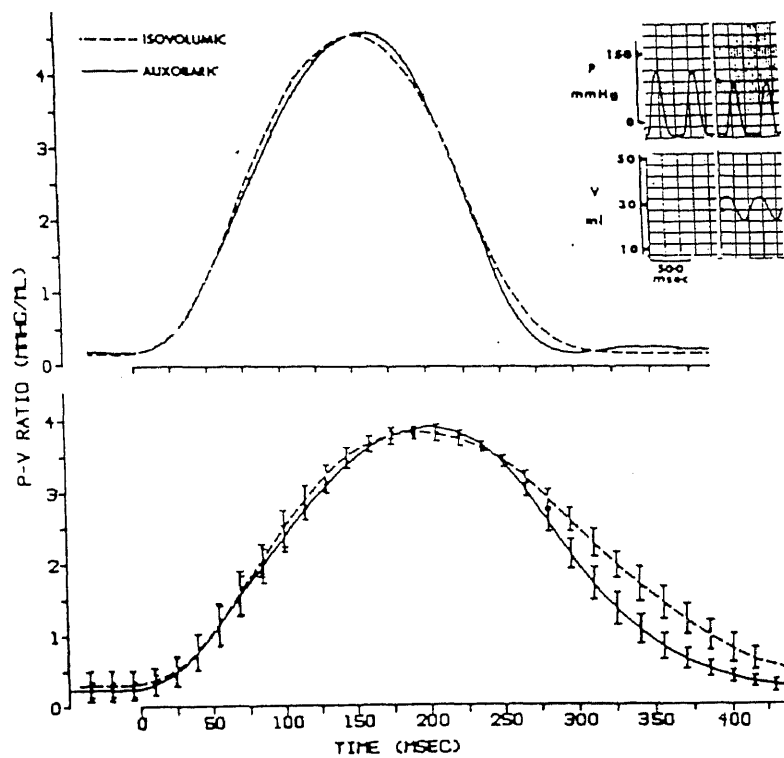
Figure 4 Two Examples of Superimposed Tracings of the Time-Varying
Pressure-Volume Ratio, E(t), of the Left Ventricle Contracting
Auxobarically for the Control Contractile State. Top: Mean E(t)
curves from six consecutive beats contracting with the same end-
diastolic volume in one ventricle. Bottom: Two mean E(t) curves,
each of which is a mean of five mean E(t) curves obtained from
differently preloaded beats in one ventricle of another dog. The
vertical barsindicate standard deviation.

2.3 Uniformity of E(t) Curves

Regardless of the considerable changes in E_{max} and T_{max} associated with the changes in contractile state, the basic shape of the systolic part of the pressure-volume ratio curve appeared to be unaffected by the inotropic intervention (Figure 5). To examine this condition more closely, the size of the E(t) curves were normalized, disregarding loading conditions or contractile state, so that their E_{max} and T_{max} would both be unity. There was only an insignificant variation in the systolic part of the normalized E(t) curve among the 103 sets of beats for the different contractile states and the different modes of contraction. Also there was little variation in the normalized curves among different preparations.

There is much supportive evidence in earlier publications for the load-independence of E_{max}, or the end-systolic pressure-volume relationship [29]. The steady state pressure-volume loop in an ejecting contraction mode reaches the isovolumic end-systolic pressure-volume relationship curve determined for the same contractile state. Although Taylor [34] reported that the force-length loop did not reach the isometric force-length relationship curve, he studied transient beats while the loading condition was continuously changing from one beat to another. Many studies have shown that it takes some time for the contractile state to reach a steady state after a step change in loading conditions. The relatively small effect of heart rate on E_{max} also has supportive evidence. Many investigators [17, 18] have shown that the peak isovolumic ventricular pressure and the end-systolic pressure-volume relationship are little affected by changes in heart rate. The shortening of T_{max} with an increase in the heart rate is also consistent with their observations.

Table 1 Effects of Enhanced Inotropism on E_{max} and T_{max}

	Control	Enhanced inotropism	P^*
Heart rate (beats/min)	119 ± 20	124 ± 37	
E_{max} (mm Hg/ml)			
I	3.65 ± 0.54	6.12 ± 0.82	0.001
A	3.58 ± 0.73	5.95 ± 1.05	0.001
$P^†$	0.9	0.2	
T_{max} (msec)			
I	167 ± 15	152 ± 17	0.02
A	184 ± 28	171 ± 26	0.02
$P^†$	0.01	0.005	

Enhanced inotropism was induced by infusing isoproterenol or norepinephrine (0.2 µg/min) into the coronary artery. I = isovolumic mode and A = auxobaric mode.

* t-Test comparison between the control and the enhancement data.

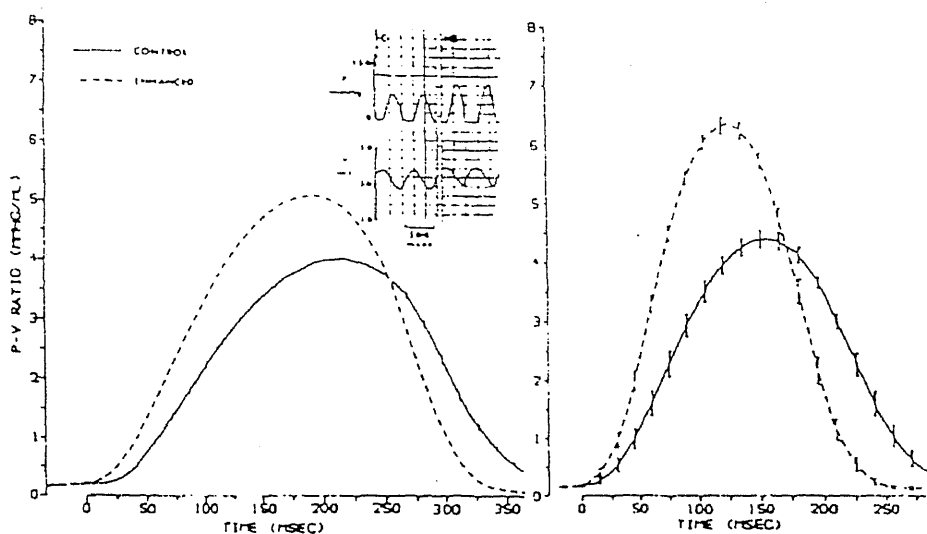† t-Test comparison between the isovolumic and the auxobaric data in the same ventricle.

Figure 5 Two Examples of Superimposed Tracings of the Time-Varying Pressure-Volume Ratio, E(t), of the Left Ventricle for the Control Contractile State (C) and the Enhanced Contractile State Induced by Norepinephrine (NE) Infusion. Left: Mean E(t) curves each from six consecutive auxobaric beats at a given end-diastolic volume and contractile state in one heart. The original pressure and volume curves are shown in the insert. Right: Mean E(t) curves each representing the mean of five mean E(t) curves from differently loaded beats under one of the specified contractile states in one preparation from another dog. The vertical lines indicate standard deviation.

One interpretation of the time-varying pressure-volume relationship is that the ventricular wall has a time-varying elasticity. At a given time in systole, the ventricle can be considered to have an actively augmented elasticity which is represented by the slope of the pressure-volume relationship curve at that time. The magnitude of this elasticity is then considered to increase and decrease with time in proportion to the rotation of the pressure-volume plane. E(t), which represents the time course of the changing slope of the pressure-volume relationship curve in this analysis, therefore represents the time-varying elasticity of the ventricular wall.

Elzinga and Westerhof [23] could not find in papillary muscle a time-varying elasticity similar to that observed in the ventricle and suggested that the ventricular time-varying elastance may be related to the complex organization of myocardial fibers in the wall, rather than to basic myocardial properties. Based on these results, they concluded that viscoelastic models are inappropriate for heart muscle, casting a doubt on the validity of the time-varying elastance model of the left ventricle.

However, their results did show the existence of a time-variant force-length relationship in the myocardium; their instantaneous pressure-volume relation of a theoretical ventricle constructed from their myocardial force-length relation data shifted upward to the left in a parallel manner during systole rather than rotating counterclockwise around a pivot of an unstressed length, and the end-systolic relation was reached at a varying end-systolic time. Although such a time-varying pressure-volume relation could be modeled by the viscoelastic model that was found not applicable to skeletal muscle, it can alternatively be modeled by a nonlinear time-varying elastance. In the time-varying elastance model, a gradual shift of the instantaneous pressure-volume relation, regardless of whether it is linear or not and

regardless of the type of shift, is theoretically associated with a gradual increment in elastic potential energy [25]. Although the time-varying elastance model and the viscoelastic model may appear similar in structure, there is a marked difference in the behavior of elasticity in the two models.

The simple time-varying elastance model has a single elastic element whose elastance gradually increases with contraction. In contrast, the viscoelastic model consists of an elastic element and a viscous element to damp the elastic element. The elastance of this elastic element increments stepwise rather than gradually at the onset of contraction, and the viscous element damps what would otherwise be a step force increment. This difference in the mechanical behavior of the two models results in a significant difference in the energetic properties.

In the time-varying elastance model, the total mechanical energy generated by each contraction depends on the time course of the pressure-volume trajectory. In other words, even when the ventricular contraction starts with the same end-diastolic volume, the total mechanical energy is instantaneously generated on the rapid increase in the elastance, and its amount is constant and, hence, independent of the time course of the shortening from a given initial length. However, the amount of external mechanical work depends on the time course of the shortening. The difference between the constant total mechanical energy minus the variable external mechanical work is dissipated as heat in the viscous element. This particular source of heat production does not arise in the simple time-varying model because it has no viscosity. Even when the time-varying elastance is partially damped by a viscous element [16], the slightly damped time-varying elastance model is still completely different from the viscoelastic model in terms of energetics, as long as the time-varying elastance model reasonably

simulates the mechanics and energetics of the left ventricle as a whole [19]. The time-varying elastance, E(t) for the ventricles has been realized in our simulation using the FNC blocks of TUTSIM as shown in Figure 6. Figure 7 shows the elastance curves for the left and right ventricles used in our model.

The following equations describe the model of the circulatory system and form a basis for our simulation. Refer to Figure 2. Since the circulatory system is a closed loop, we can start at any point in the loop. Starting at the Pulmonary Arterial Compartment and proceeding clockwise around the loop, we can write:

1) Pulmonary Arterial System

$$\frac{d}{dt}(PAP) = 0.0325 \left[90 \left(PRV - PAP\right) - 13 \left(PAP - PCP\right) \right] \tag{5}$$

where PAP is the pulmonary arterial pressure, PRV the pressure in the right ventricle, PCP the pressure in the pulmonary capillaries. 90 (PRV - PAP) is the flow from the pulmonic valve and 13 (PAP - PCP) is the flow out of the pulmonary arterial system. The resistance values (i.e., (1/90) and (1/13)) and the capacitance value (i.e., (1/0.0325)) are estimated from normal resting flow and volume data available in standard Physiology texts (10), where values for a dog are given. They have been extrapolated to a 70 kg man.

2) Pulmonary Capillary System

$$\frac{d}{dt}(PCP) = 0.09 \left[13 \left(PAP - PCP\right) - 7 \left(PCP - PVP\right) \right] \tag{6}$$

where PVP is the pressure in the pulmonary venous system, and 7 (PCP - PVP) is the flow out of the pulmonary capillary system.

3) Pulmonary Venous System

$$\frac{d}{dt}(PVP) = 0.005 \left[7 \left(PCP - PVP\right) - 25 \left(PVP - PLV\right) \right] \tag{7}$$

where PLV is the pressure in the left ventricle, and 25 (PVP - PLV) is the flow out of the mitral valve.
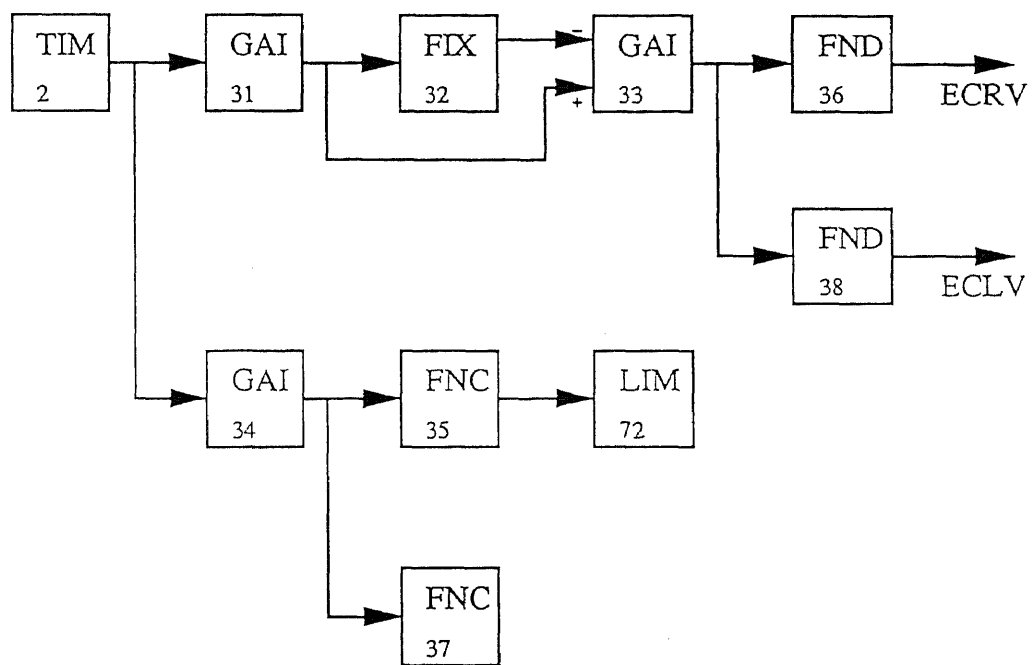
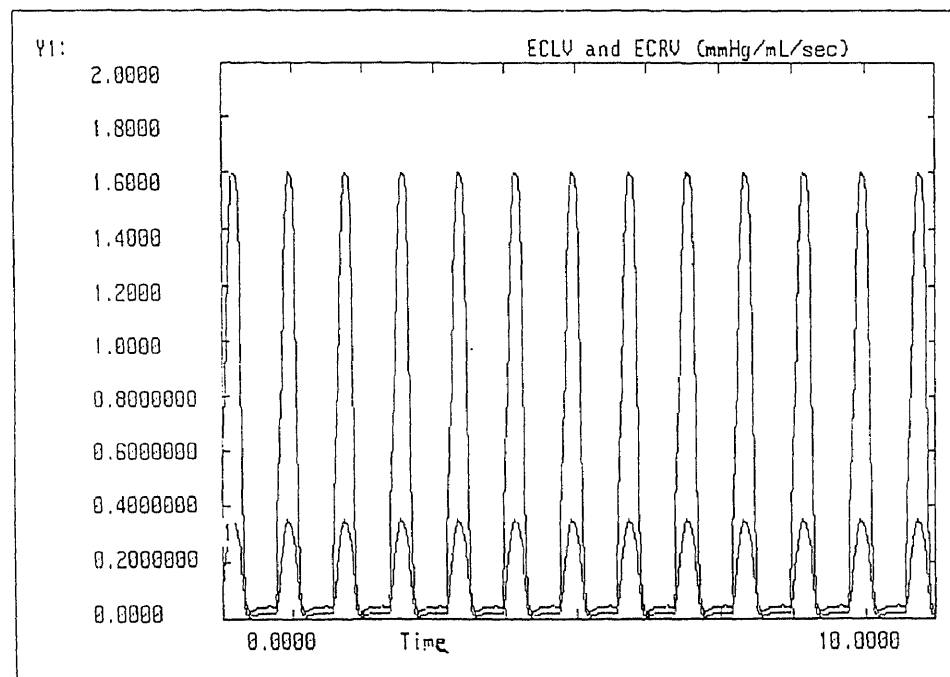Figure 6 TUTSIM Realization of the Left and Right Ventricular Elastances

Figure 7 The Time Varying Elastance Curves for the
Left and Right Ventricles Used in the Model

4) Left Ventricle

$$\frac{d}{dt}\left(\frac{PLV}{ECLV}\right) = \left[25\,(PVP - PLV) - 50\,(PLV - PAO)\right] \tag{8}$$

where PAO is the aortic pressure, ECLV is the elastance of the left ventricle, and 50 (PLV - PAO) is the flow out of the aortic valve.

5) Aorta

$$\frac{d}{dt}(PAO) = 1.0\left[50\,(PLV - PAO) - 17.182\,(PAO - PLA)\right] \tag{9}$$

where PLA is the pressure in the large arteries, and 17.182 (PAO - PLA) is the flow out of the aorta.

6) Large Arteries

$$\frac{d}{dt}(PLA) = 0.240\left[17.182\,(PAO - PLA) - 0.0427\,(PAO - PVC) - 2.0953\,(PLA - PAA)\right] \tag{10}$$

where PVC is the pressure in the vena cava, PAA the pressure in the arterioles, 0.0427 (PAO - PVC) is the flow in the coronary circulation, and 2.0953 (PLA - PAA) is the flow out of the large arteries.

7) Arterioles

d/dt (PAA) = 1.15 [2.0953 (PLA - PAA) - 0.384 (PLA - PLV*)

$$- 0.192\ (PLA - PVU) - 3.181\ (PAA - PSC)] \tag{11}$$

where PLV* is the pressure in the large veins, PVU the pressure in the venules, 0.384 (PLA - PLV*) is the flow in the renal system (kidneys) and the hepatic artery, 0.192 (PLA - PVU) the flow in the spleen and GI tract, and 3.181 (PAA - PSC) is the flow into the systemic capillaries.

8) Systemic Capillaries

$$\frac{d}{dt}(PSC) = 0.07\left[3.182\,(PAA - PSC) - 0.128\,(PAA - PVU) - 21.477\,(PSC - PVU)\right] \tag{12}$$

where 0.128 (PAA - PVU) is the flow in the skeletal muscle, and 21.477 (PSC - PVU) the flow in the venules.

9) Venules

$$\frac{d}{dt}(PVU) = 0.05\left[21.477\,(PSC - PVU) + 0.128\,(PAA - PVU) - 171.821\,(PVU - PLV^*)\right] \quad (13)$$

where 171.821 (PVU - PLV*) is the flow in the large veins.

10) Large Veins

d/dt (PLV*) = 0.003 [171.821 (PVU - PLV*) + 0.384 (PLA - PLV*)

$$+ 0.1923\ (PLA - PVU) - 1.65\ (PLV - PVC)] \quad (14)$$

where 1.65 (PLV - PVC) is the flow in the vena cava.

11) Vena Cava

$$\frac{d}{dt}(PVC) = 0.004\left[1.65\,(PLV - PVC) + 0.03367\,(PAO - PVC) - 78\,(PVC - PRV)\right] \quad (15)$$

where 1.65 (PLV - PVC) is the flow in the vena cava.

12) Right Ventricle

$$\frac{d}{dt}\left(\frac{PRV}{ECRV}\right) = \left[78\,(PVC - PRV) - 90\,(PRV - PAP)\right] \quad (16)$$

where ECRV is the elastance of the right ventricle, 78 (PVC - PRV) is the flow out of the tricuspid valve, and 90 (PRV - PAP) is the flow out of the pulmonic valve.

Table 2 shows the resistance and compliance values for the different systems used in our model.

2.4 Myocardial Oxygen Supply and Demand

Several formulas have been suggested in the literature for estimation of myocardial energy demand and MVO_2. In 1895, Frank [20] developed a theoretic approach to describe the total effort of the heart. His formula represented a sum of five major components :

$$A = \int_{V_1}^{V_2} P\,dV - \int_{V_1}^{V_2} \Psi\,(V)\,dV + \sum\frac{dm\,v_1^2}{2} - \sum\frac{dm\,v_2^2}{2} + \frac{R}{V} \pm A_i + W \quad (17)$$

$$\text{I} \qquad\qquad \text{II} \qquad\qquad \text{III} \qquad \text{IV} \quad \text{V} \quad \text{VI} \quad \text{VII}$$

1) The energy requirements for pressure-volume work done by the ventricle during systole (I) subtracted by the pressure-volume work received by the ventricle during diastole (II).

2) The kinetic work of the heart for blood leaving the ventricle during systole (III) which is also diminished by the kinetic energy of the blood entering into the ventricle during diastole (IV).

3) The energy requirements for intramyocardial frictional resistances during contraction (V).

4) Requirements for changes of internal mechanical energy (VI).

5) Energy that is combusted for heat generated by metabolism (VII).

Although Frank's approach is interesting, the resulting formula is obviously more theoretical and not applicable to clinical or experimental measurements. Later in 1912, a more practical suggestion was made by Rhode [20], who considered the product of heart rate and systolic blood pressure to be an appropriate indirect index for myocardial oxygen demand. In contrast to Frank's formula, this so-called "rate pressure product" (RPP) was much more suitable for clinical application because blood pressure and heart rate can be measured noninvasively. In the following decades, the RPP has been advocated by several authors, with modifications. It also might be assumed that external cardiac work is also related to myocardial energy turnover. However, it was shown that external cardiac work alone does not correlate with myocardial oxygen demand. Evans and Matsuoka [22, 24] have demonstrated that the oxygen cost of the increase in flow work was less than for the same increase in pressure work. The efficiency of myocardial performance therefore is not constant, but decreases with pressure load. Subsequently, several studies focused on indices of MVO_2 based on wall tension or wall force (TTI, contractile element work, estimated wall tension,

Table 2 Resistance and Compliance Values for the Different Systems used in
the Model

System	Resistance (mmHg/mL/sec)*	Compliance (mL/sec)/mmHg*
Pulmonary Arterial System	0.011	30.7692
Pulmonary Capillary System	0.0769	11.1111
Pulmonary Venous System	0.1429	200.000
Left Ventricle	0.04	ECLV (t)
Aorta	0.04656	1.0
Large Arteries	0.0582	4.167
Arterioles	0.47724	0.8696
Systemic Capillaries	0.31428	14.2857
Venules	0.04656	20.000
Large Veins	0.00582	333.333
Vena Cava	0.01782	0.0871
Right Ventricle	0.01282	ECRV (t)
Coronary Circulation	29.7	-
Brain	8.2286	-
Kidneys	4.8	-
Hepatic Artery	18.6	-
Spleen and GI Tract	5.2	-
Skeletal Muscle	7.84	-

* Values were estimated from normal resting values for flows, pressures, and volumes in a 70 kg man. These values are available in any standard Physiology textbook [10], where only dog values are available. These have been extrapolated to the hypothetical 70 kg man.

and the triple product). It soon became evident that, in addition to wall tension, additional factors influence myocardial energy demand. It is interesting to note that more recent suggestions for estimation of myocardial energy turnover from hemodynamic variables turn back to the additive concept of Frank's formula. Bretschneider developed an additive formula based on five components contributing to total energy turnover of the myocardium. These are E_0 for basal metabolism, E_1 and E_4 for electrophysiologic processes, and E_2 and E_3 for maintenance and development of tension [26]. This formula was shown to be valid in animal experiments for a broad range of hemodynamics and also proved to be a useful tool for the analysis of pathophysiologic settings. A major drawback of this formula was the requirement of a left ventricular tip manometer for measurement of dP/d_{tmax}.

Rooke [21] introduced an approach named the pressure work index (PWI), which is an additive combination of basal metabolism, RPP, and a term containing cardiac work. In animal experiments performed by Rooke, it was found that this empiric formula was equivalent to Bretschneider's formula in predicting relative changes of myocardial oxygen consumption, and was even superior for prediction of absolute values.

Obviously, it is not possible to extrapolate from animal experiments to the human heart. RPP and TTI might be suitable for rough estimation of relative changes of myocardial oxygen demand in patients. The additive formula of Bretschneider is not directly applicable to patients because new constants must be developed. In principle, it could be possible to determine the necessary constants K_0 through K_4 from the measured patient data by statistical methods, with a multilinear regression analysis. However, this kind of calculation is not well suited for the current Eg data because the

number of measurements and the limited variability of inotropic states in patients does not allow determination of the unknown constants with sufficient accuracy.

In contrast, more data are available for calculation of PWI, and only three instead of five constants are to be determined. It is therefore possible to calculate new constants retrospectively for PWI by a multilinear regression. The results of such a fitting procedure are shown in Figure 8. A linear regression coefficient of r = 0.84 and constants of 0.02 for K_0, 8.37. 10-4 for K_1 and 8.0. 10-6 for K_2 were found (Figure 8). The formula of the PWI was slightly modified for clinical use (PWI_{mod}). The term "SV * HR * BW-1" of the original formula was replaced by cardiac index (CI (L/min * m^2)), which is used more commonly in patients than cardiac output per kilogram of body weight. The true accuracy of PWI_{mod} is shown in Hoeft's work [1] on myocardial oxygen demand.

With respect to the application of PWI_{mod} in anesthetized patients, the relation between PWI_{mod} and MVO_2 has been shown by Hoeft [1]. The mean differences between PWI_{mod} and MVO_2 and the corresponding standard deviations and 95% confident limits for the mean differences were calculated for the awake state for measurements obtained during anesthesia. No major systematic difference was found with respect to anesthetic state or surgical stimuli, which confirms the results of Rooke [21] obtained in dogs. Therefore, it seems that estimation of myocardial oxygen demand by PWI_{mod} is not affected by anesthesia. The main advantage of PWI_{mod} in comparison with E_g is the availability of necessary data in many critically ill patients. The PWI_{mod} formula:

$$PWI_{mod} = E_0 + E_1 + E_2 \qquad (18)$$

where,
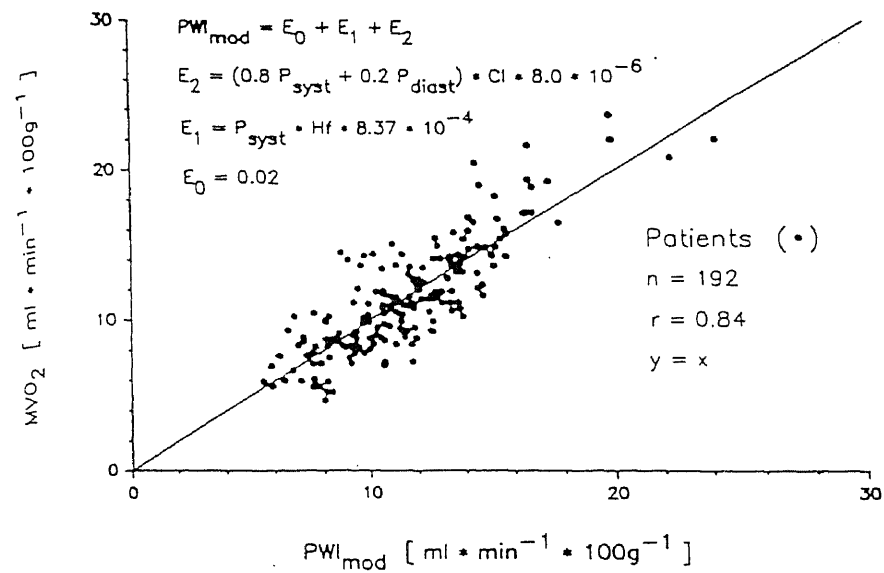
Figure 8 Multilinear Regression Analysis of a Modified Pressure Work Index
(PWI$_{mod}$) and Myocardial Oxygen Uptake (MVO$_2$) in Patients. For
clinical application, cardiac index (CI) was used instead of cardiac
output, divided by body weight. New constants were calculated by a
multilinear regression fitting procedure.

$$E_0 = 0.02 \tag{18 a}$$

$$E_1 = P_{sys} * HR * 8.37 * 10^{-4} \tag{18 b}$$

$$E_2 = (0.8 * P_{sys} + 0.2\, P_{dia}) * CI * 8.0 * 10^{-6} \tag{18 c}$$

where P_{sys} is the systolic pressure, P_{dia} the diastolic pressure, CI the cardiac index, and HR the heart rate.

The coronary vasculature is represented by a fixed resistance. The coronary blood flow (CBF) is predicted from the integrated difference between the aortic and left ventricular pressure divided by the coronary resistance. Myocardial oxygen supply is predicted from the coronary blood flow and an assumed myocardial extraction ratio for oxygen:

$$O_2\ \text{supply (mL/min)} = CBF * (O_2\ \text{extraction ratio}) * (O_2\ \text{in blood}) \tag{19}$$

where O_2 extraction ratio = 0.95 and O_2 in blood by volume % = 19.0

The coronary blood flow is realized in the simulation as shown in Figure 9. The output of block 33 is a sawtooth waveform developed using blocks 2, 31, 32, and 33. The gain of block 31 determines the period of the sawtooth waveform. The SGN block (98) requires a waveform that has some values in the negative region, so that the output of the SGN block would be -1 or +1 depending on the input. This is the region behind the use of a constant block (97) which subtracts a small portion of the waveform such that the output of the SUM block (96) is a waveform with a few of its values in the negative region. The resetable integrator RIN (99) gives the integrated difference of the aortic and the left ventricular pressures for each cardiac cycle.

2.5 TUTSIM Simulation Language

A high level language is devised to liberate the user from the details of programming, thus permitting the user to focus his attention to solve the
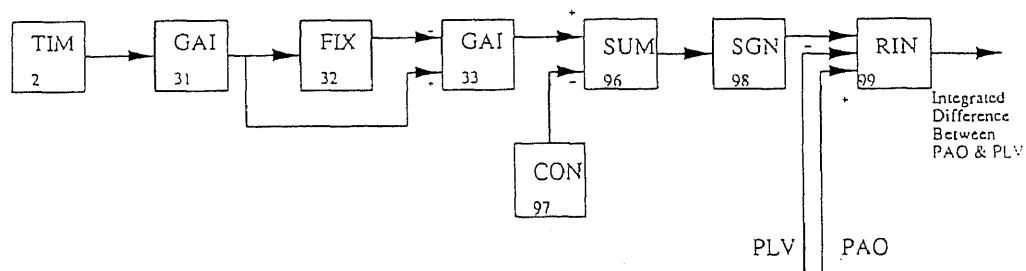
Figure 9 TUTSIM Realization of Obtaining the Integrated Difference Between Aortic and Left Ventricular Pressure Waveforms

problem. In the early 1960's, analog computers had their own simple way of doing just that.

They were usually programmed from a block diagram sketch and a list of equations representing the system being modeled. The analog computer, by definition, "solved" a problem by substitution of functional electrical analog blocks for real functions. Thus the block diagram of the real system and the block diagram for wiring up the analog computer were pretty much the same diagram.

Soon digital computers outpaced analog computers in speed, accuracy and economy. However the high level languages they brought in were modeled more to the inner working of the computer than to the realities of the problems that needed solutions. Most simulation programs followed these techniques, and often wound up incomprehensible to the practising engineer, more than the computer languages themselves.

TUTSIM has re-established the analog between the real world systems and the computer model language. It has the convenience of an analog computer and the speed and accuracy of the digital computer. Furthermore, interaction with the user, and convenience of use are enhanced by the availability of TUTSIM on the popular microcomputers of today.

2.5.1 Simulation to Describe Real Time System Behavior

Real time system behavior is usually represented by linear and nonlinear differential equations. The solutions of these equations are possible only by "continuous simulation", which can be realized by using TUTSIM. these solutions can describe the movements and energetics of all the complex physiologic systems.

2.5.2 Simulation with TUTSIM

The biggest advantage of using TUTSIM is that the user does not have to be concerned about computer algorithms. However the user must be able to determine the applicable equations of the system under consideration. TUTSIM blocks represent mathematical operations. TUTSIM block diagrams may be written from the equations term by term, or sometimes by direct inspection of the real system.

The flow is simply:

Problem :---> Mathematical Model :---> Block Model :---> Results

Model parameters such as the initial values of an integration are easily entered and changed. results are usually time dependent values and are available in graphical display or numerical tables on the screen or as hard copy.

Non-linear, discontinuous, and special mathematical blocks increase the power of TUTSIM far beyond the analog computers. The core of TUTSIM is written in assembly language. This allows for the fastest possible program execution and thus achieve "continuous simulation" of real time systems. Figure 10 shows the block diagram used in the simulation.
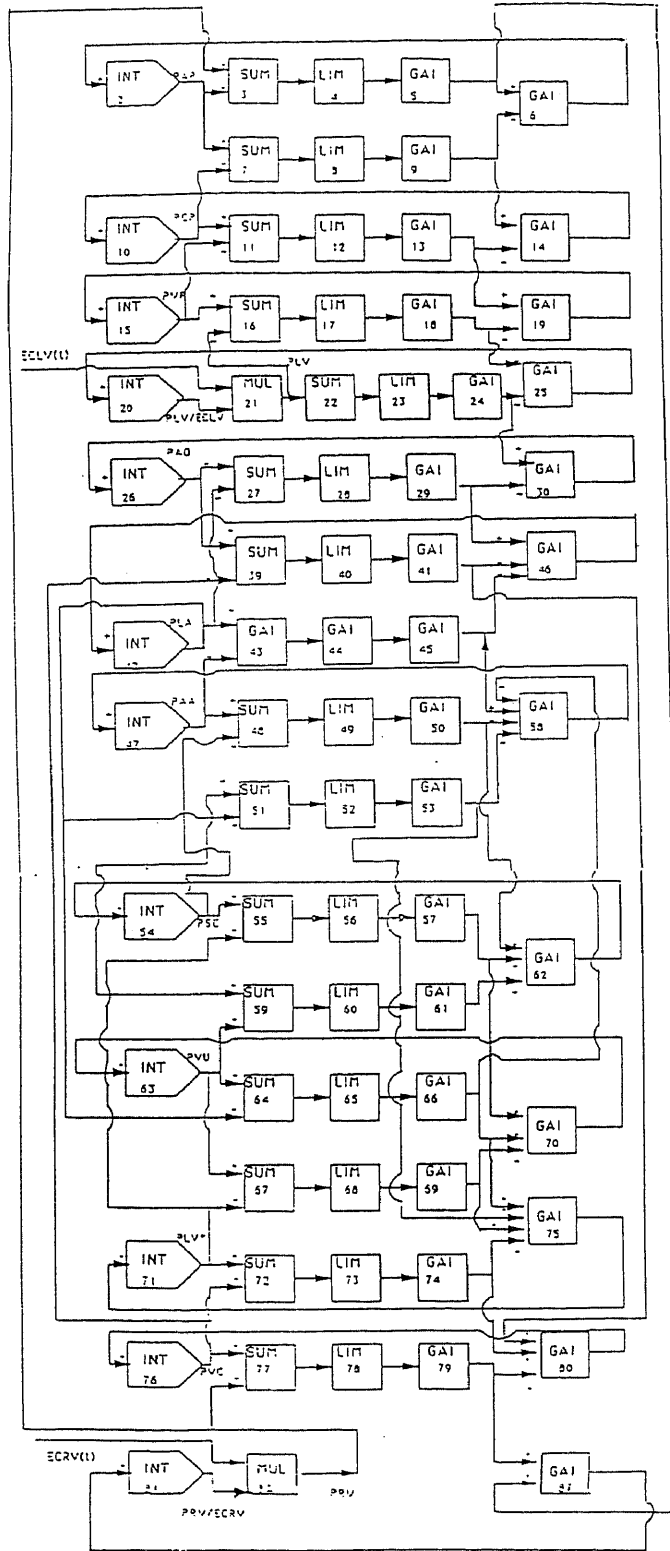
Figure 10 TUTSIM Realization of the Cardiovascular System

CHAPTER 3
RESULTS AND DISCUSSION

3.1 Results and Discussion

Simulation results include predictions of aortic and left ventricular pressure waveforms (Figure 11), the left ventricular pressure-volume curve (Figure 12), pressures, volumes, flows, and myocardial oxygen supply and demand in the various compartments can be computed.

The model predicts that with normal values for the cardiovascular parameters and a fixed coronary vascular resistance that cannot dilate to meet increased demand, myocardial oxygen supply is 80.44% greater than myocardial oxygen demand. The model makes predictions for cardiac mechanics and myocardial oxygen supply and demand in humans. By adjusting several of the cardiovascular variables simultaneously, the model can be used to simulate specific clinical conditions.

3.2 Cardiac Mechanics

The model predicts left ventricular and aortic pressure waveforms for a cardiac cycle (Figure 11). The left ventricular pressure-volume loop is also plotted for the whole cardiac cycle (Figure 12). The model predicts pressures, volumes, and flows which closely correlates with those values in basic cardiovascular physiology. Appendix B shows the pressures, volumes, and flows associated with the model.

The model produces results consistent with well-known concepts of basic cardiovascular physiology. Raising the left ventricular end-diastolic pressure increases the cardiac output (Figure 13), confirming the model's ability to predict the Frank-Starling effect. Myocardial depression (E_{max} = 25% normal)

36
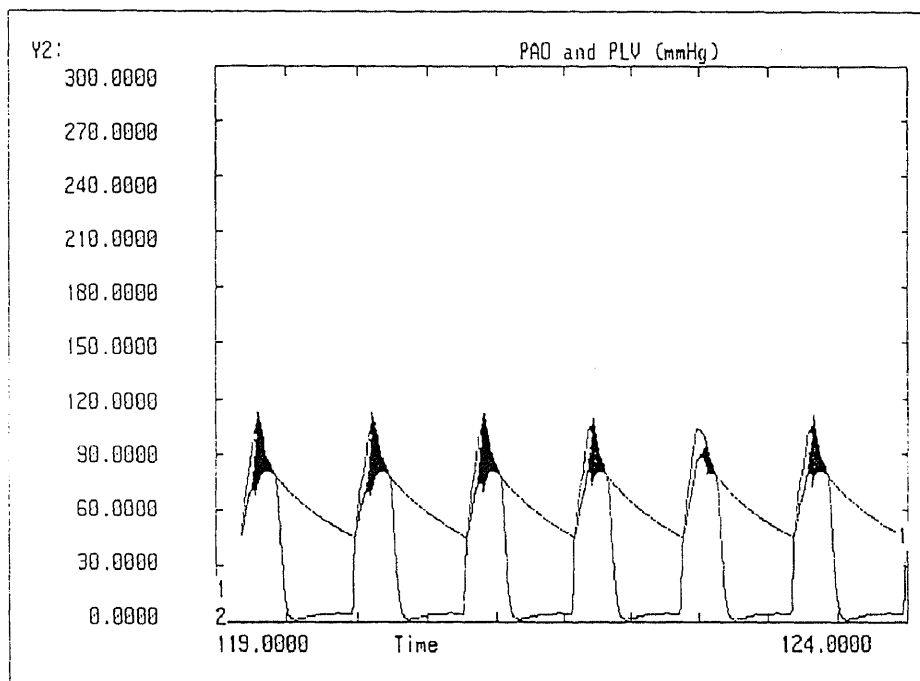
Figure 11 Aortic and Left Ventricular Pressure Waveforms against Time
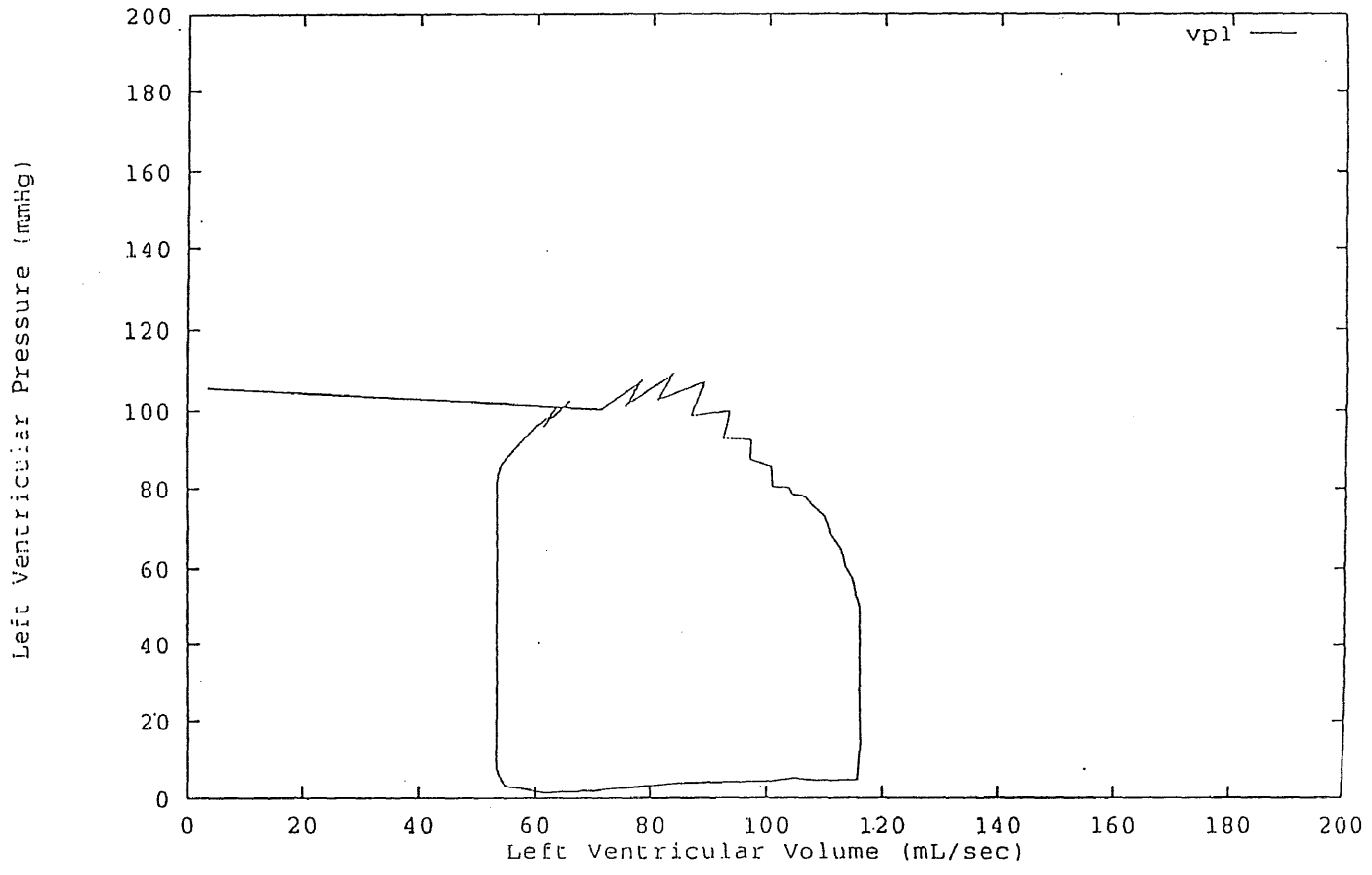
Figure 12 Pressure-Volume Diagram for the
Normal Case with Heart Rate = 75 beats/min
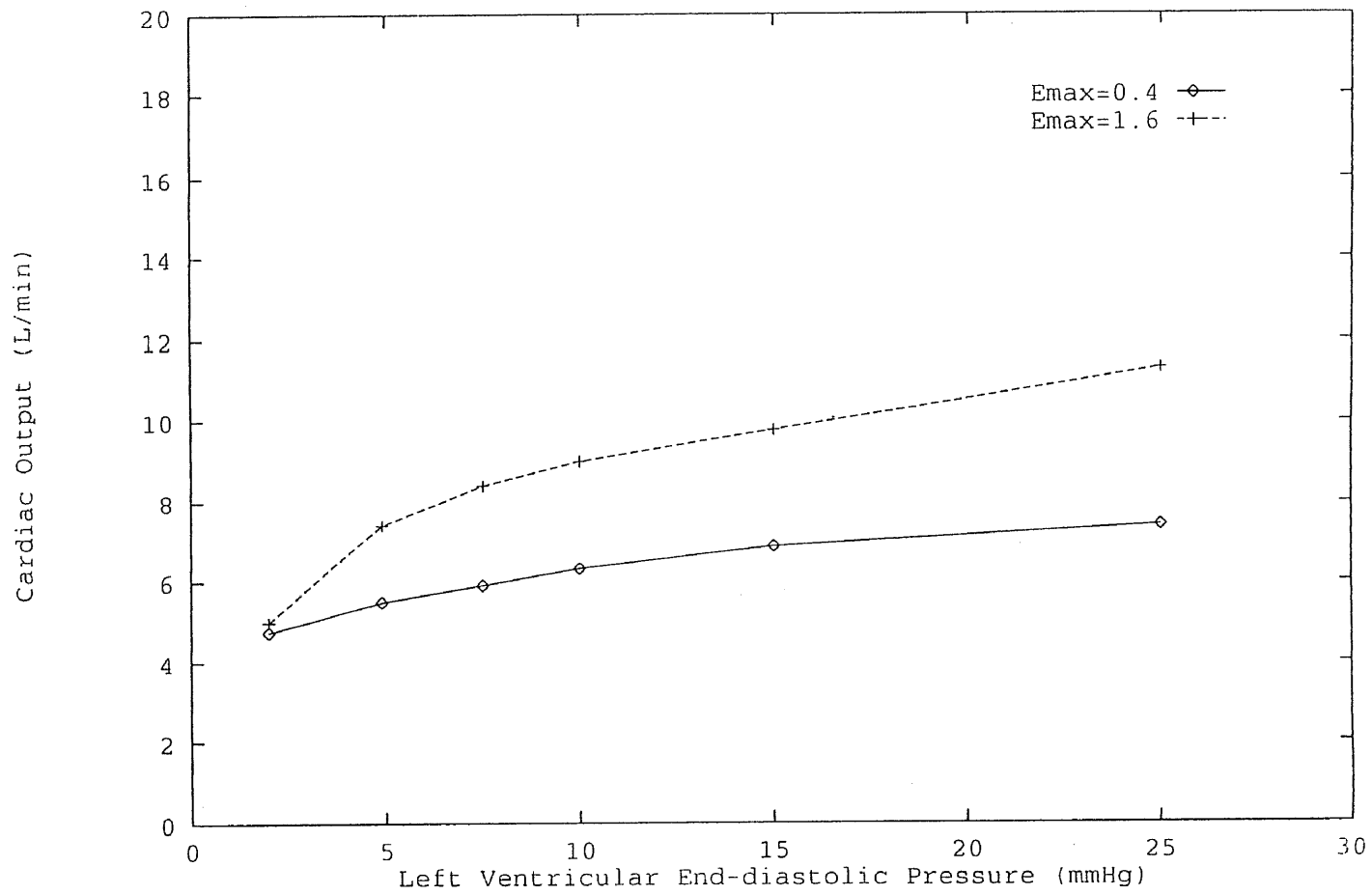
Figure 13 Relationship between Left Ventricular
End-Diastolic Pressure and Cardiac Output

shifts the filling pressure-cardiac output curve to the right which is consistent with the pathophysiology of the failing left ventricle (Figure 13).

Some simulations were performed to study the effect of changing hemodynamic parameters on myocardial supply and demand. Figure 14 shows the relationship between left ventricular elastance and myocardial oxygen supply and demand. As the contractility (E_{max}) is increased, myocardial oxygen supply and demand increases. The simulation predicts that the increase in myocardial oxygen supply is sufficient to meet the increased demand. It should be realized, however, that in the present model, cardiac blood flow is calculated using the mean aortic pressure, rather than diastolic pressure. This will overestimate cardiac blood flow. The pressure-volume curve for E_{max} = 0.8 and E_{max} = 3.2 are shown in Figures 15 and 16. Figure 17 shows that as the systemic vascular resistance is raised the myocardial oxygen demand increases, but the oxygen supply increases more to avoid ischemia. The pressure-volume curve for SVR = 0.7483 and SVR = 0.1909 are shown in Figures 18 and 19.

Some important insights could be drawn from the model simulated. The effect of some commonly used cardiovascular drugs on cardiac output and other hemodynamic variables can be estimated from the model. It is known that the major effect of drugs on the cardiovascular system is in alterations of cardiac output, heart rate, contractility, and peripheral resistance. These parameters are easily altered in the model, to simulate the action of various drugs on cardiac output and systemic hemodynamics.

For example, the combination of cardiac stimulation (150% normal), decreased venous compliance (67% normal), and decreased arteriolar resistance (67% normal) produces a large increase in cardiac output (170% normal). The decreased venous compliance modulates the fall in preload and
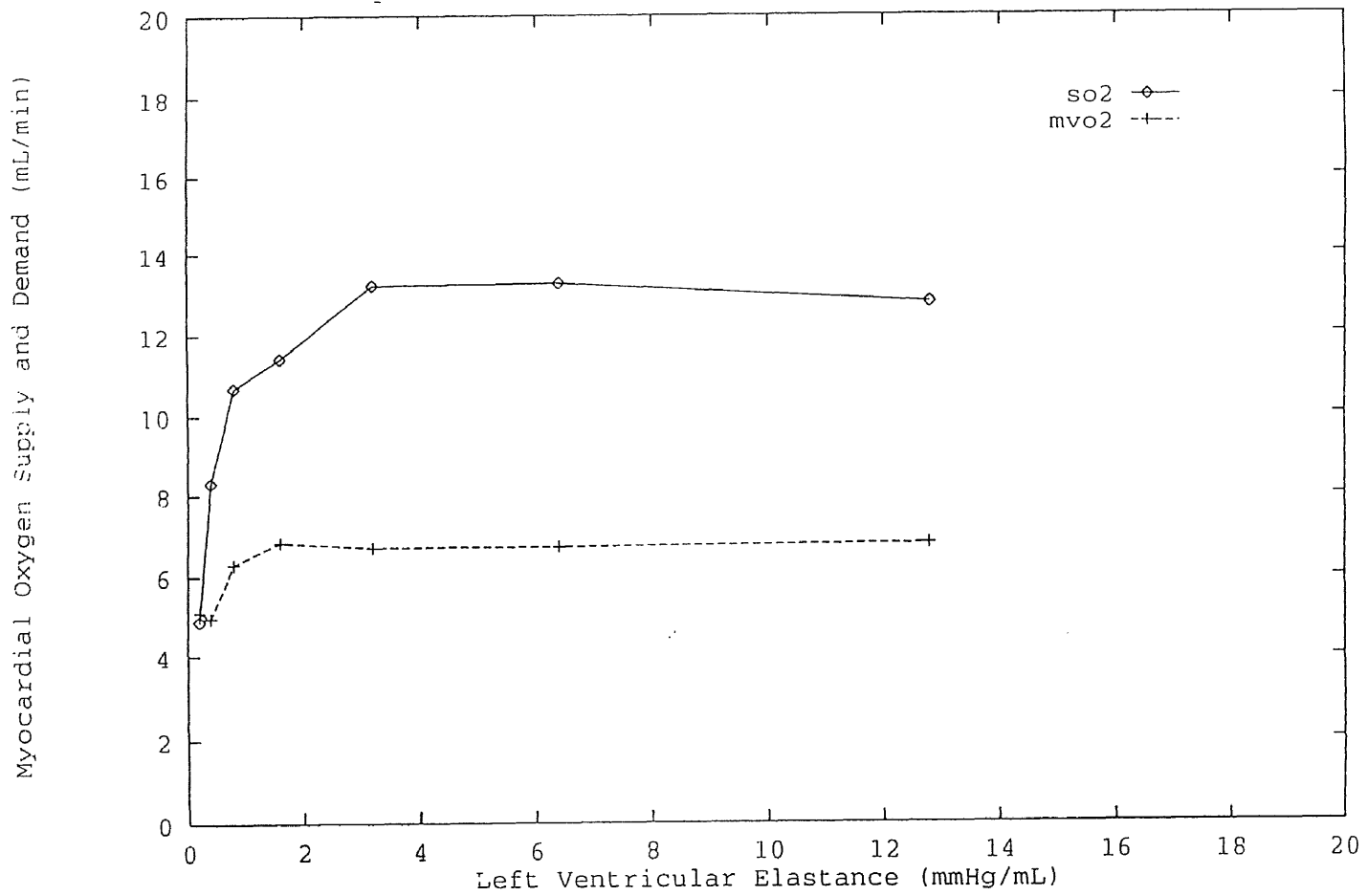
Figure 14 Relationship between Elastance and
Myocardial Oxygen Supply and Demand
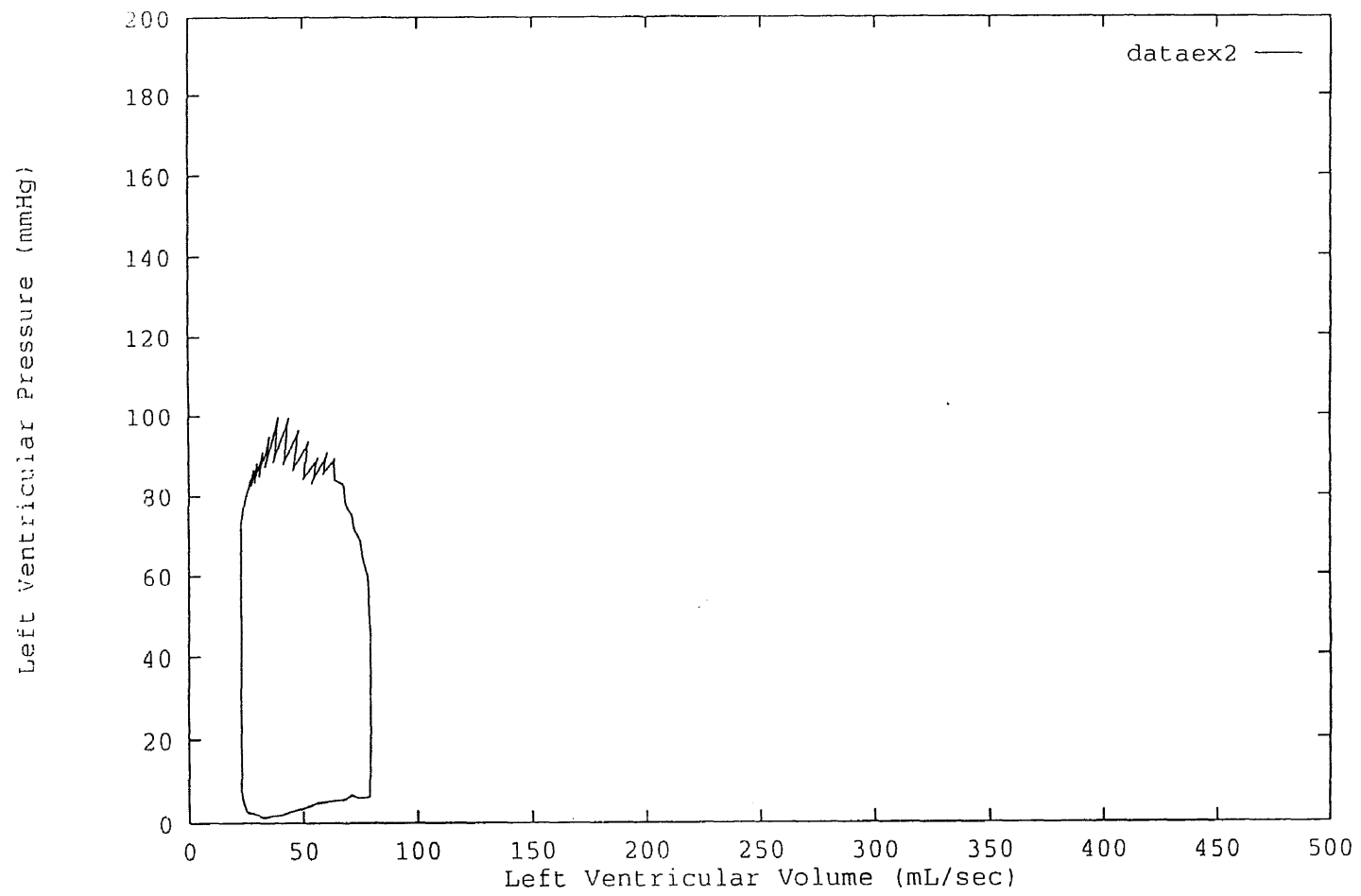
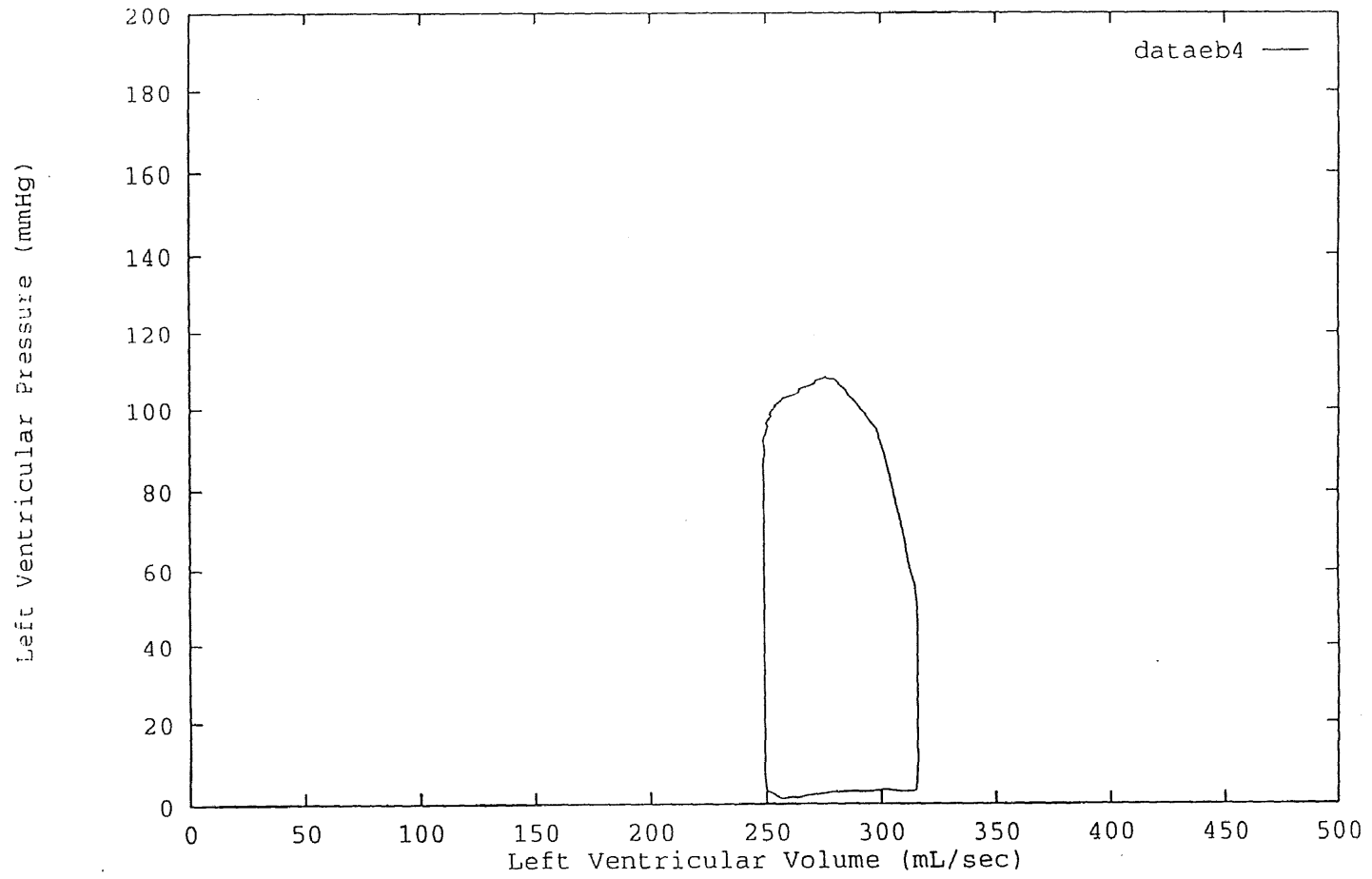**Figure 15** Pressure-Volume Diagram for $E_{max} = 0.8$

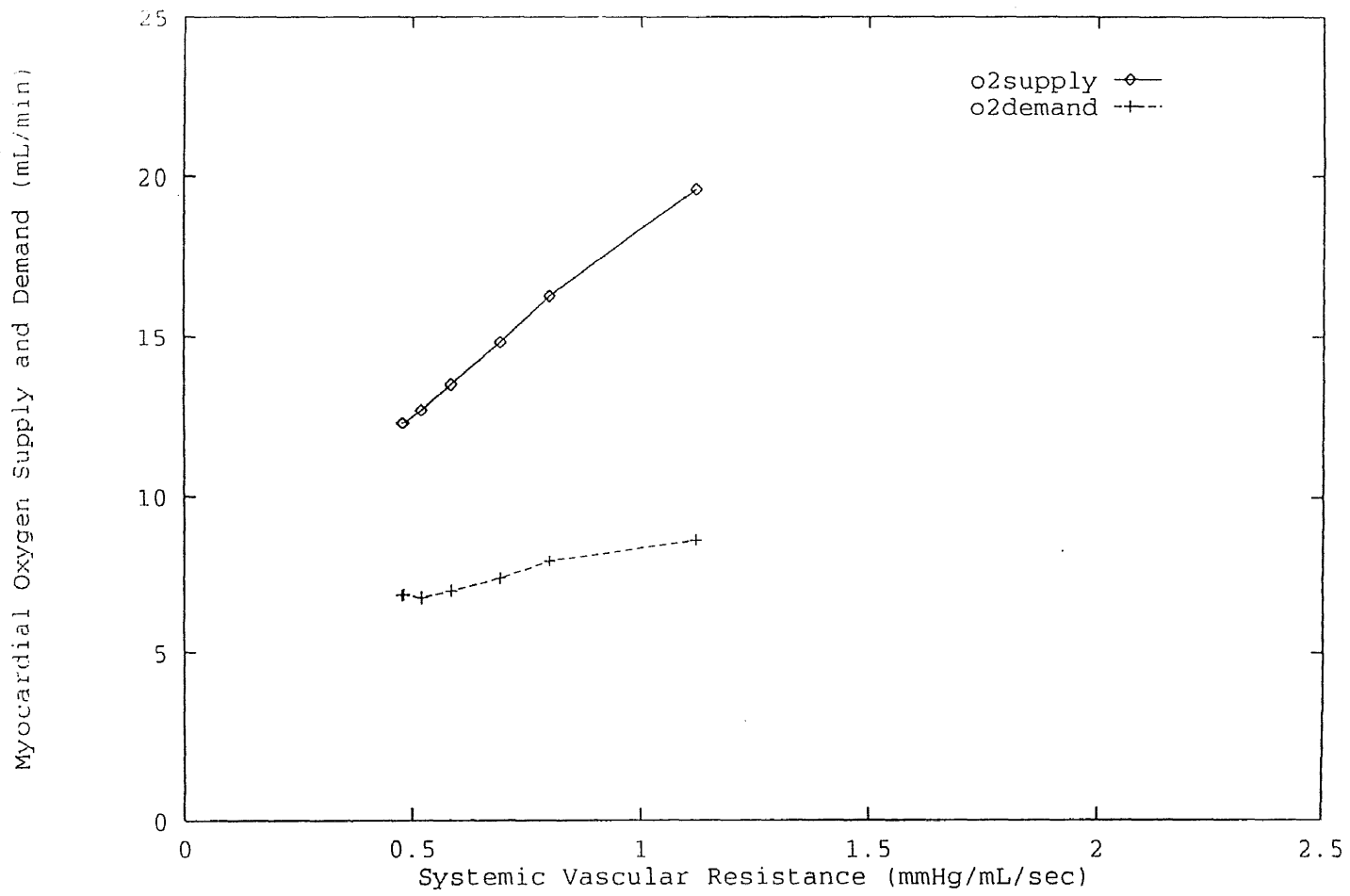**Figure 16** Pressure-Volume Diagram for E_{max} = 3.2

Figure 17 Relationship between Systemic
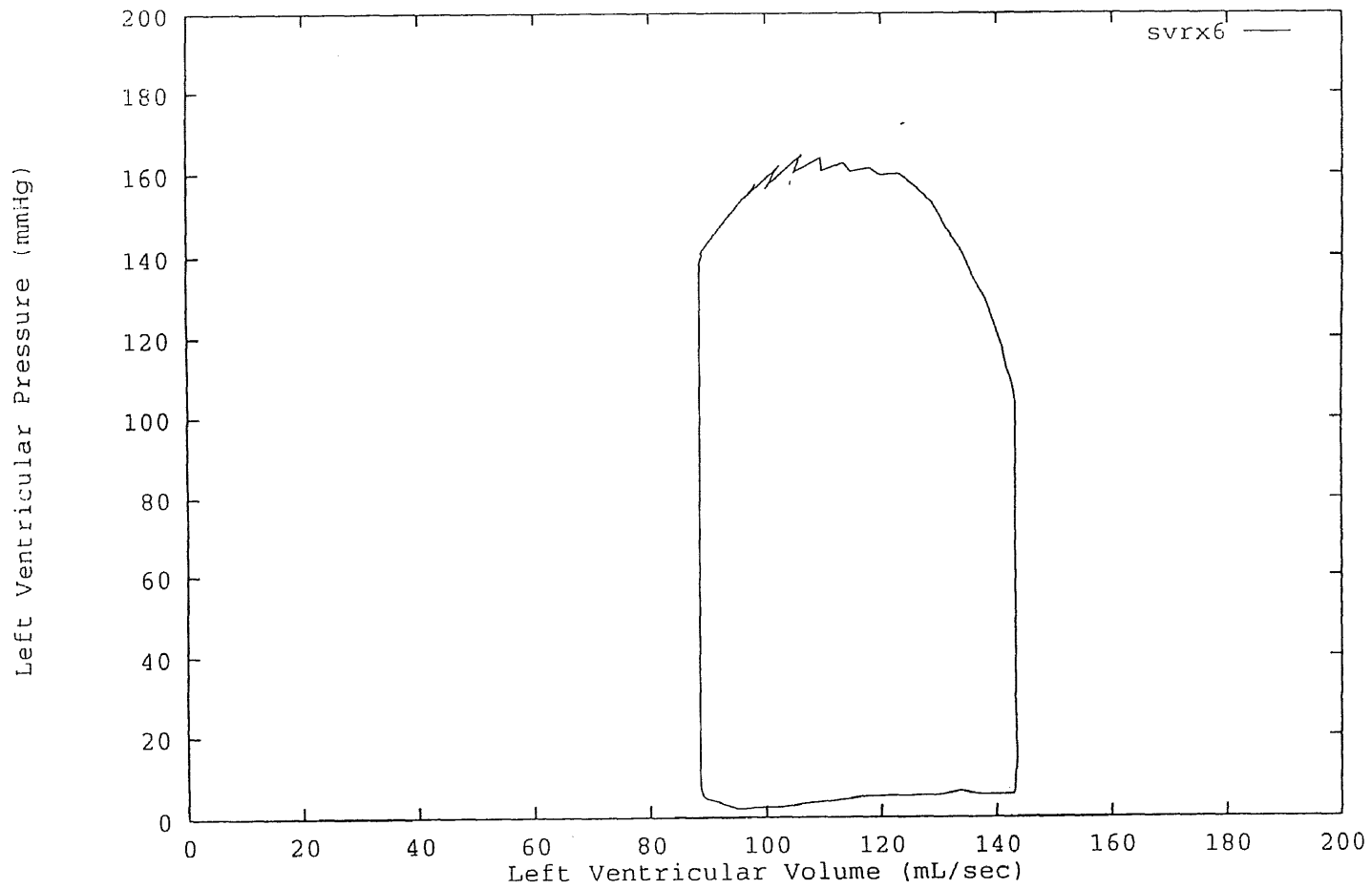Vascular Resistance and Cardiac Output

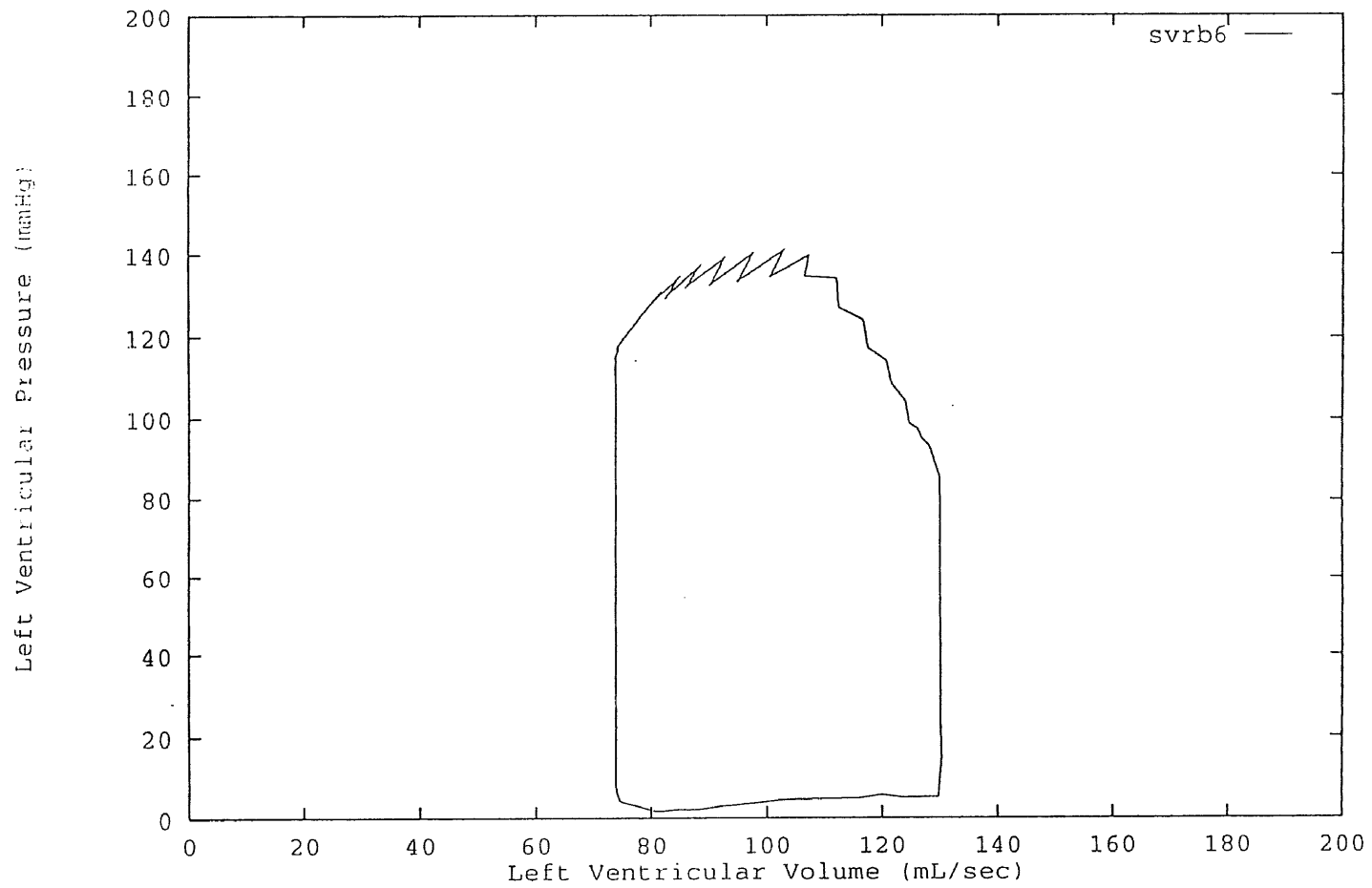**Figure 18** Pressure-Volume Curve for Systemic
Vascular Resistance = 0.7483

Figure 19 Pressure-Volume Curve for Systemic
Vascular Resistance = 0.1909

the decreased arteriolar resistance modulates the increase in afterload that normally follow cardiac stimulation alone. These combined effects resemble the effect of epinephrine. Thus, simultaneous changes in several variables that change cardiac output in the same direction, produces larger changes in cardiac output than the sum of their individual effects. Conversely, simultaneous changes in several semi-independent variables that change cardiac output in opposite directions, tend to neutralize one another, resulting in no change in cardiac output. The decrease in cardiac output produced by an increase in peripheral arteriolar resistance can be neutralized by a simultaneous decrease in venous compliance. This reflects an increase in myocardial oxygen supply because myocardial oxygen supply is affected by changes in cardiac output. As shown in Figure 17 there is not much increase in myocardial oxygen demand.

Table 3 shows the effect of epinephrine and norepinephrine and Table 4 shows the effect of isoproterenol and phenylephrine on various hemodynamic parameters. The changes in these data could be used to predict changes in myocardial oxygen supply and demand.

3.3 Regulation of Heart Rate

In all of the above simulations, the heart rate was kept constant. Several clinical conditions could be simulated if the heart rate could be varied. Work is in progress for observing the changes in myocardial oxygen supply and demand, as a result of changes in heart rate along with other hemodynamic parameters. The following section delineates a method for changing the heart rate that could be incorporated into the existing cardiovascular model.

Figure 20 illustrates the basic baroreceptor feedback loops. The top half represents the relation between arterial blood pressure (ABP) and heart rate

Table 3 Actions of Epinephrine and Norepinephrine on the Variable Expressed as Percent of Control Value

Dose	Epinephrine			Norepinephrine		
	0.25	0.5	2.0	0.25	0.5	2.0
	$\mu g / kg / min$			$\mu g / kg / min$		
Blood volume	100	100	100	100	100	100
Arterial compliance	100	100	100	?	?	?
Splanchnic venous compliance	60	40	30	70	50	40
Muscle venous compliance	90	80	70	90	80	70
Other venous compliance	?	?	?	?	?	?
Pulmonary artery compliance	?	?	?	?	?	?
Pulmonary venous compliance	?	?	?	?	?	?
Ventricular diastolic compliance	?	?	?	?	?	?
Splanchnic arteriolar resistance	50	60	80	130	150	200
Muscle arteriolar resistance	50	70	100	160	250	400
Renal arteriolar resistance	150	200	250	160	250	400
Other arteriolar resistance	100	100	100	130	150	200
Splanchnic venous resistance	100	100	100	120	130	150
Muscle venous resistance	100	100	100	150	200	300
Pulmonary resistance	?	?	?	100	100	100
Heart rate	120	130	140	120	130	140
Right ventricular contractility	120	130	140	120	130	140
Left ventricular contractility	120	130	140	120	130	140
Atrial contractility	120	130	140	120	130	140
Thoracic pressure	?	?	?	?	?	?

Table 4 Actions of Isoproterenol and Phenylephrine on the Variables
Expressed as Percent of Control Value

Dose	Isoproterenol			Phenylephrine		
	0.25	0.5	2.0	2	4	16
	µg/kg/min			*µg/kg/min*		
Blood volume	100	100	100	100	100	100
Arterial compliance	?	?	?	?	?	?
Splanchnic venous compliance	70	65	60	90	80	70
Muscle venous compliance	100	100	100	95	90	80
Other venous compliance	100	100	100	?	?	?
Pulmonary artery compliance	?	?	?	?	?	?
Pulmonary venous compliance	?	?	?	?	?	?
Ventricular diastolic compliance	?	?	?	?	?	?
Splanchnic arteriolar resistance	60	40	30	120	135	170
Muscle arteriolar resistance	80	50	40	140	160	200
Renal arteriolar resistance	90	80	60	150	175	220
Other arteriolar resistance	80	50	40	120	135	170
Splanchnic venous resistance	?	?	?	?	?	?
Muscle venous resistance	?	?	?	?	?	?
Pulmonary resistance	100	100	100	100	100	100
Heart rate	120	130	140	100	100	100
Right ventricular contractility	140	150	160	100	100	100
Left ventricular contractility	140	150	160	100	100	100
Atrial contractility	140	150	160	100	100	100
Thoracic pressure	?	?	?	?	?	?
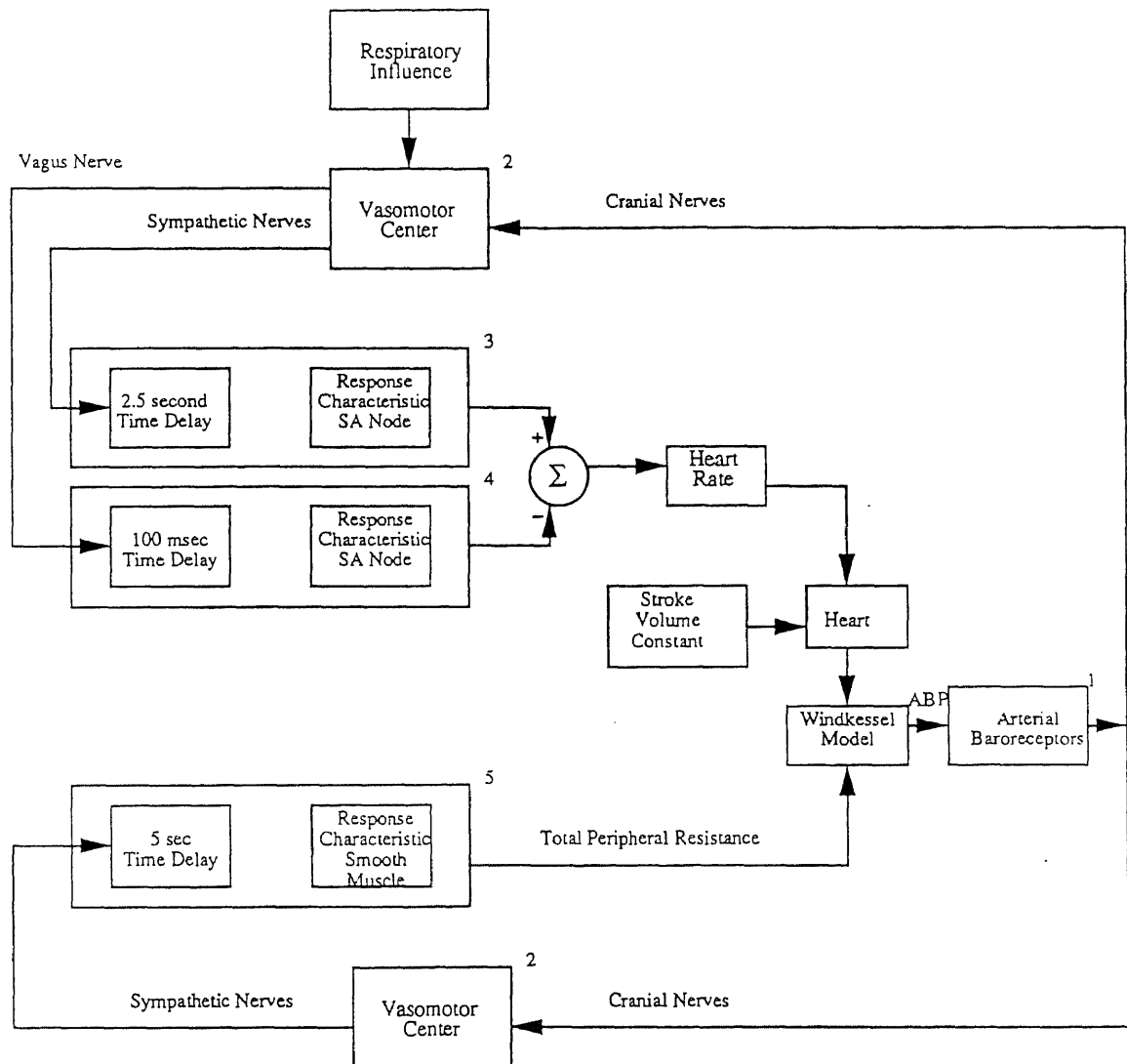
Figure 20 Block Diagram for Baroreceptor Regulation of
Heart Rate and Total Peripheral Resistance [17]

(HR); the bottom half represents the relation between ABP and total peripheral resistance (TPR). The arterial baroreceptors (block 1) respond such that a rise in ABP acutely increases the number of impulses per second, which are transmitted by the carotid sinus (originating from the carotid sinus) and the aortic depressor (originating from the aortic arch) nerves. These nerves terminate in the nucleus tractus solitarius (block 2). The signal acts to return ABP to its control value by altering HR and TPR through changes in autonomic nerve activity acting on the cardiac pacemaker and vascular smooth muscle cells [28]. The reflex delay between arterial baroreceptor stimulation and the onset of the efferent nerve activity is in the order of 100-300 ms [29].

The sympathetic nerves leave the spinal cord (Figure 20 bottom), and the output of the α-adrenergic effector mechanism (block 5 in Figure 20) alters total peripheral resistance. In the model, the arterial baroreceptors respond to changes in ABP (Figure 21), and the output of the α-adrenergic effector mechanism mediates the targeted changes in TPR. The targeted value of TPR that the arterial baroreceptors would achieve if pressure were held constant. Therefore, if ABP is held constant and the cardiovascular control system is allowed time to respond, the targeted values would be achieved. In practice the targeted TPR would not be achieved, since the arterial baroreceptors are constantly responding to changes in blood pressure. For each targeted TPR value, the α-adrenergic effector mechanism (block 5) is capable of altering TPR. The output of block 5 describes the α-adrenergic effector mechanism's influence on TPR. An increase in stimulation of the sympathetic nerves from the vasomotor center causes an increase in smooth muscle contraction and thus TPR. Contraction begins 5 seconds (5000 ms) after stimulation and reaches maximal contraction 15 seconds later [30]. The resistance is modeled
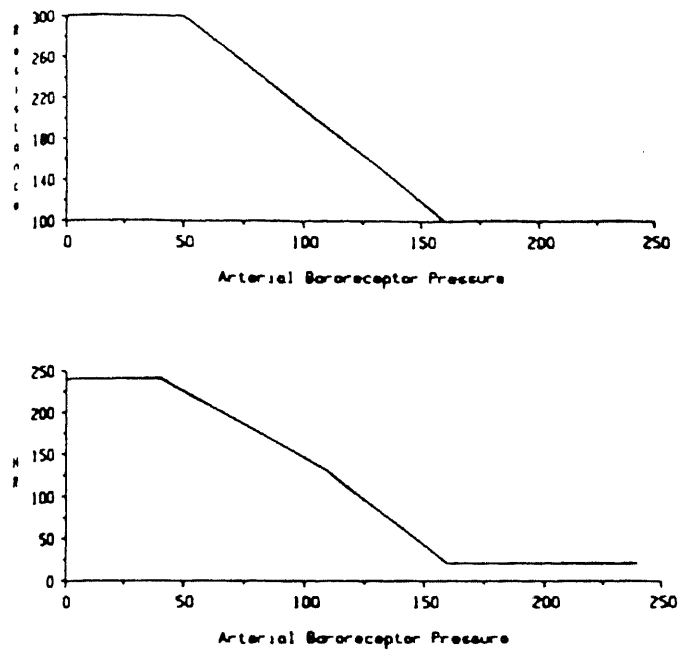
Figure 21 Arterial Baroreceptor Stimulus Response Curve. Relationship between mean arterial blood pressure and targeted total peripheral resistance in arbitrary units (top) and targeted heart rate (HR) in beats/min (bottom)
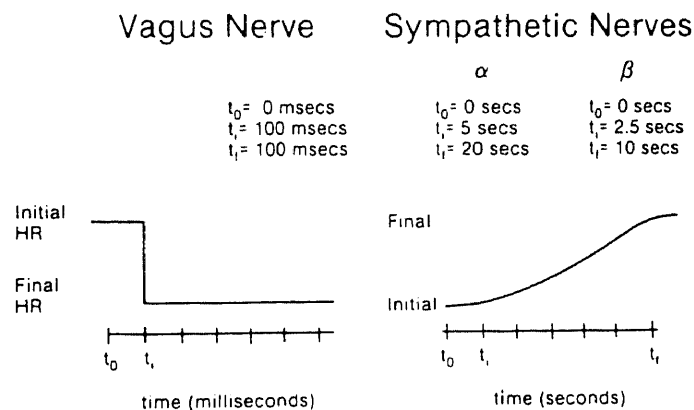
Figure 22 Response Characteristic of Vagal (left) and Adrenergic (right) Effector Mechanisms After a Step Increase in Neural Stimulation Rate

to increase linearly with time in response to a step increase in sympathetic nerve activity (Figure 22).

The vagus nerve leaves the motor nuclei that are located in the regions of the nucleus of the vagus; the sympathetic preganglionic nerve fibers leave the spinal cord and pass by way of the stellate and caudal cervical ganglia. In the model, the β-adrenergic (block 3) and vagal (block 4) effector mechanisms alter heart rate as described in Figure 23, and the outputs of the effector mechanisms sum to create the targeted HR. The targeted HR is that value of HR that the arterial baroreceptors would achieve if pressure were held constant. Therefore, if ABP is held constant and the system allowed to respond, the targeted value would be achieved. In practice, the targeted HR would not be achieved since the arterial baroreceptors are constantly responding to changes in blood pressure. For each targeted HR value, the vagal effector mechanism is capable of slowing the heart rate, whereas the β-adrenergic effector mechanism is capable of accelerating the heart rate.

The effects of vagal and β-adrenergic effector mechanisms in the regulation of HR cannot be described in terms of a linear summation since their interaction in the regulation of HR is complex. Madwed et Al [31] have attempted to account partially for this vagal-adrenergic effector mechanism interaction in the curves labeled N in Figure 23. At rates < 60 beats/min, a further decrease in HR is mediated by the output of vagal effector mechanism alone. This interaction is consistent with the finding that sympathetic activity is low during basal conditions and that propranolol causes a small decrease in HR during base line states [32]. At heart rates > 180 beats/min, a further increase in rate is mediated by the output of the β-adrenergic effector mechanism (Figure 23). This interaction is consistent with the finding that
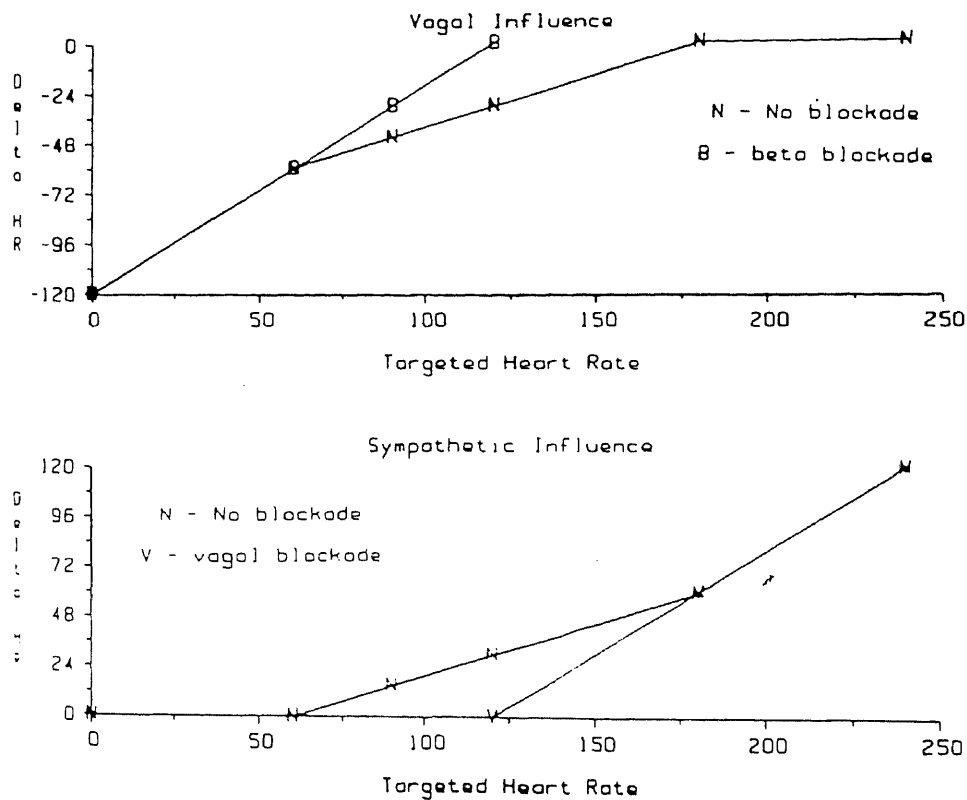
Figure 23 Concept of Vagal and Sympathetic Control of Heart Rate (HR). Role
of vagal and β-adrenergic effector mechanisms on a change in HR from initial
HR (HR$_{initial}$). Output of vagal effector mechanism is capable of slowing HR;
output of β-adrenergic effector mechanism is capable of accelerating the HR.

vagal inhibition with glycopyrrolate accelerates the mean heart rate to about 180 beats/min during baseline states [32].

The output of block 3 describes the β-adrenergic effector mechanism's influence on the heart rate. Stimulation causes an increase in HR. Heart rate begins to increase 2.5 sec (2500 ms) after stimulation and reaches a maximal HR 7.5 sec later. The HR is modeled to increase linearly with time in response to a step increase in sympathetic activity (Figure 22). the output of block 4 describes the vagal effector mechanism's influence on HR. Stimulation causes a decrease in HR. Heart rate decreases 100 ms after stimulation and persists at that HR throughout stimulation (Figure 22) The output of the β-adrenergic and vagal effector mechanisms are then added together to give an actual HR value (HR_{actual}). This is represented in the following manner:

$$HR_{actual} = HR_{initial} + \gamma\, HR_{vagal} + \delta\, \Delta\, HR_{sympathetic}$$

where ΔHR_{vagal} and $\Delta HR_{sympathetic}$ are the changes in HR targeted by the vagal and sympathetic inputs to the heart (Figure 23). $HR_{initial}$ is the rate (120 beats/min) of a completely denervated heart. ΔHR_{vagal} and $\Delta HR_{sympathetic}$ could only be achieved if the level of neural input was held steady for a sufficiently long time. The dynamics of the change are incorporated in the coefficients γ and δ, which vary from 0 to 1 according to the time course illustrated in Figure 22.

When the output of vagal effector mechanism is blocked, only the output of the β-adrenergic effector mechanism can alter HR. The HR cannot decrease below 120 beats/min but can increase above 120 beats/min (Figure 23). When the output of β-adrenergic mechanism is blocked, only the output of the vagal effector mechanism can alter the HR. The HR cannot exceed 120 beats/min but can decrease below 120 beats/min (Figure 23). Therefore, the effector outputs, HR and TPR, are mediated by the output of the vagal, and β-

adrenergic effector mechanism. The net result of an increase in carotid sinus pressure is reduced sympathetic tone and enhanced vagal tone, which tends to decrease ABP towards its original value. Thus changes in efferent vagal activity and efferent sympathetic activity induced by the arterial baroreceptor system have a variety of effects on the heart and arterial vasculature.

4.1 CONCLUSIONS

The described model combines accepted models of the cardiovascular system and calculates myocardial oxygen supply and demand. The model represents an important step in understanding the hemodynamic determinants of myocardial oxygen supply and demand. Predictions of the model agree with experimental and clinical observations and provide useful insights into the role of contributing variables that are difficult to manipulate in real life. Given normal values for cardiovascular parameters, the model predicts acceptable values for cardiac output, blood volumes and flows. In addition, predicted myocardial oxygen supply and demand agrees with published values. The predicted aortic and left ventricular pressure waveforms have characteristic morphology. The left ventricular pressure-volume curve is also characteristic in its appearance. The Frank-Starling effect is predicted quite accurately for normal and depressed contractility. The effect of systemic vascular resistance on myocardial oxygen supply and demand is in accordance with the published, with larger effects on stroke volume for the ventricle with poor contractility. The model predicts that as the systemic vascular resistance is increased, the myocardial oxygen supply increases more, improving the oxygen balance. This is in agreement with previous reports that hypotension worsened ischemic dysfunction in the presence of a severe stenosis. The model also predicts that higher mean arterial pressure is required to avoid myocardial ischemia with increased contractility.

Competition exists between the heart and the rest of the body. The cardiovascular variables cannot be manipulated to optimize myocardial oxygen balance while ignoring cardiac output. Myocardial oxygen balance is most favorable with elevated systemic vascular resistance, reduced E_{max}, and reduced left ventricular end-diastolic pressure. But this leads to an

unacceptably low stroke volume. Animal studies have demonstrated that in the presence of a coronary stenosis, an increase in left ventricular end-diastolic pressure improves cardiac output at the expense of aggravated myocardial ischemia, while an increase in systemic vascular resistance reduces cardiac output but may improve myocardial ischemia [34].

There are several other factors that influence myocardial oxygen supply and demand that have not yet been simulated. The effect of heart rate on myocardial oxygen balance was not studied, though the idea was conceptualized. In conclusion, this dynamic model could be used to correlate the action of drugs on myocardial oxygen supply and demand as a result of a change in one or more of the hemodynamic determinants of myocardial oxygen balance.

APPENDIX A

This section documents the exact syntax of the TUTSIM operators. Many blocks have "parameters". These are the constant coefficients for the functions. Often these parameters represent the real physical values of a model like resistances, capacitances, etc. Hence the user is well advised to use consistent values. Undefined parameters default to zero.

1) **ABS**olute Value Block
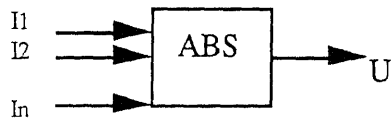
U(t) = Absolute value of the algebraic sum of inputs, ΣIn

The ABS block has no parameters, but it should have at least one input.

2) **CON**stant Function Block
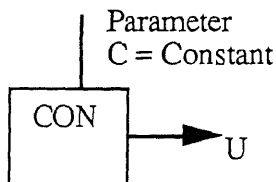
U(t) = Constant

The CON block has one parameter and no input.

The constant is a parameter that can be changed quickly by the "CP", Change Parameter command. Thus if the constant represents a physical design factors, it may be changed and the model run again to determine the effect of the particular design change.

3) Filed **DAT**a Input Block
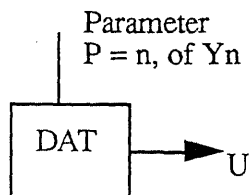
With the DAT block, recorded information from a file on a disk may be used as input. The file to be used should be in the same format created by the "SF", Start simulations with results to an ASCII file, command. In this file, the time and up to four Y outputs can be stored. One of the Y recordings will be the input to the DAT block. The Y recording is selected with the parameter. The input is time synchronized with the time recorded in the "first column" of the file. If necessary, interpolation and extrapolation will be used. After starting a simulation run with a model that includes a DAT block, TUTSIM will prompt for the filename which contains the DAT block information. At that time, the filename is to be typed. The DAT block should have one parameter and no inputs.

4) DELay Function Block

Parameters
Rn = Resolutoin in time units
Td = Delay time
Ic = Initial condition
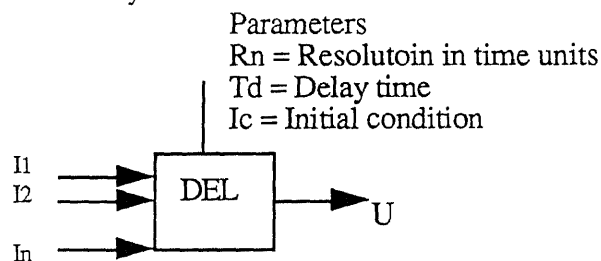
$U(t) = \Sigma In \left(t - T_d \right)$ if time $\geq T_d$; otherwise $= I_c$

$U(0) = I_c$

DEL gives out the input value at T_d time ago. This is in units of the simulation time value, not just steps. Resolution is the alloted time interval between stored elements. It is unreasonable to make this less than the delta t step time of the simulation. The actual number of stored values is

Stored values = (Delay time) / (Resolution time)

and cannot be larger than 1000. If the resolution is larger than a delta time step, output values are interpolated. The DEL block should have at least one

input and three parameters. If the third parameter is not specified, the initial condition default to zero.

5) FIX Function Block
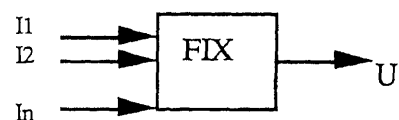
U(t) = Integer value of algebraic sum of inputs, ΣIn

The output of the FIX function block is the largest absolute integer not greater than the absolute sum of the inputs, i.e. truncation is performed. The FIX block has no parameters, but should have at least one input.

The range of nearly 2, for inputs $-1 < \Sigma In < 1$, will convert to zero.

6) FuNCtion Generator Block;
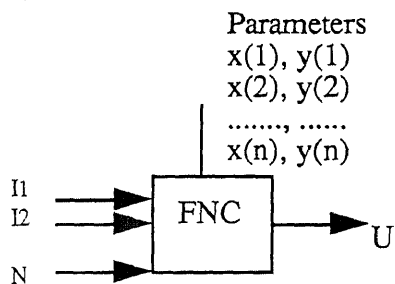
U = F(x), where $x = \Sigma In$; and $x(n) < x(n+1)$

x may lie outside of the range of x(1) and x(n). N is the number of x, y pairs.

Any arbitrary piecewise-linear function may be described. The values 1, X(1), Y(1), ..., n, X(n), Y(n) are entered as parameters. Or the values may be in an ASCII file and entered during the change parameter command. As with all blocks, the structure must be defined first. The value "n" is the number of X, Y pairs, and is entered as the last value on the structure input line. There may not be a comment with the FNC block. During parameter entry, or in the data file, n is 1, 2, 3, ... And the condition X(n) < X(n+1) must be maintained at all times. Otherwise TUTSIM will refuse to allow further parameter entry for this or for other blocks until the condition is corrected.

A FNC block should have a minimum of 3 parameter pairs, and a maximum of 100 parameter pairs. There should be at least one input, and the last of the input string is actually the number of X, Y pairs.

Manual parameter entry:

In the "change parameter" command, give the FNC block number and <cr>. TUTSIM will answer with a list of all parameters, zero or otherwise. Then start entering sequences of three values:

n, X(n), Y(n) <cr>

Filed data parameter entry:

First prepare a text data file with exactly n three value lines like the above. Then in "change parameters" start as with the Manual parameter entry. When asked if you wish to enter filed data, answer with "F". You will be asked for the filename. Then the file will be read into the FNC parameters. As with all the blocks, if the structure of that block is changed, the parameters for that block reset to zero.

7) FuNction Duplicator Block

Parameters
P = Existing FNC
Block number
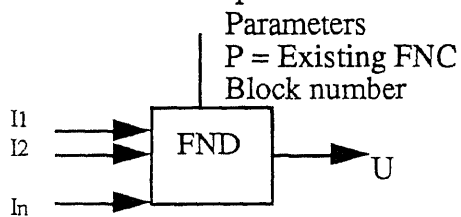
U = F(x), where x = ΣIn

(x) is the function defined by an existing FNC block whose block number is P, the FND block parameter. The block numbered P must exist or the simulation will be cancelled by an error message. the FND block is useful as a shorthand parameter. If the same function is used more than once in a model, then describe it just once with a FNC block, and duplicate it with the FND block as needed elsewhere.

8) GAIn Block

Parameters
P = Gain

GAI ⟶ U
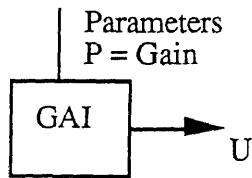
$U(t) = P * \Sigma In$

Usually P is the physical value in the model. This block should have a minimum of one input and one parameter.

9) INTegrator Function Block

Parameter
Ic = Initial condition

I1
I2   INT ⟶ U
In
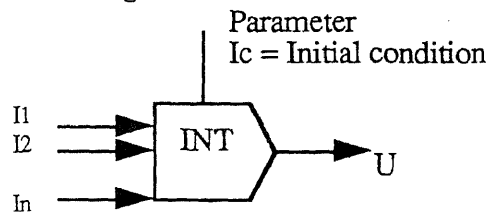
$$U(t) = \int \Sigma In$$

The output of this block is the integral, with respect to time, of the sum of the inputs. INT produces the integral as an Adams-Bashforth second order integration step. INT integrator produces the most accurate approximations for "smooth" input functions. However, for discontinuous or abruptly changing inputs, the "EUL" integrator will give superior results during the region of discontinuity.

10) LIMit Function Block

Parameters
min = minimum
max = maximum

I1
I2   LIM ⟶ U
In

$U(t) = \Sigma In, \quad min \leq \Sigma In \leq max$

$= min < \Sigma In < min$

$= max > \Sigma In > max$
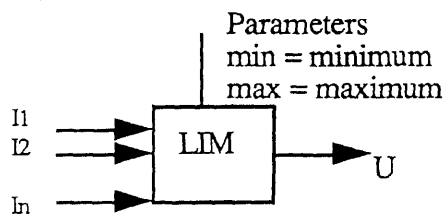
The limit block has 2 parameters, with Min < Max. The limit block should have at least 1 input. The order of the parameters should be noted. This function sums the inputs, then applies the Min/Max logic.

11) Arithmetic MULtiply Block
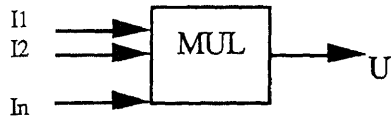
$$U(t) = I_1 * I_2 * I_3 * ..... * I_n$$

MUL may have any number of inputs but a minimum of 2 inputs. It does not have any parameters.

12) The REMark Block
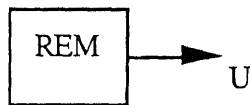
The REM block allows lengthy comments in a model listing. The REM block has no mathematical or computational function. It does however have a block number and will be listed in the block order of a model listing. Up to 240 characters of comment may be assigned to a REM block. Since the REM block has no inputs and no outputs, it would hardly appear in the block diagram. The assignment of a block number does allow the comment to be held in the model data structure. The REM block , like any other block may be added or changed at any time.

13) Resetable INtegrator Function Block

Parameter
Ic = Initial condition
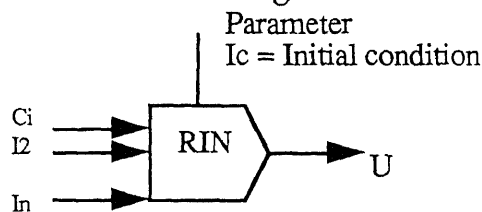
$$U(t) = \int \Sigma In \text{ , while Ci = TRUE}$$

At time = 0, and while Ci = FALSE

$U(0, Ci = F) = Ic$

The RIN integrator is an INT type integrator, except it may be reset to the initial condition anytime by setting the control input FALSE (negative). The RIN block has one control input and at least one signal input. The control input Ci must not come from a history block. If the model requires such a connection, a GAI block is used in place (K = 1) between the controlling block and the RIN control input. Also negating the control input may lead to indeterminate results.

14) SiGN of Inputs Function Block

I1
I2   SGN
In   U
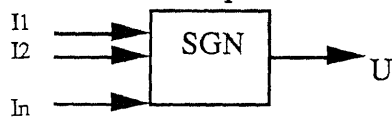
$U(t) = 1 \geq \Sigma In \geq 0$

$U(t) = -1 < \Sigma In < 0$

The output is positive or negative one, carrying the sign of the input.

15) SUM Function Block

I1
I2   SUM
In   U
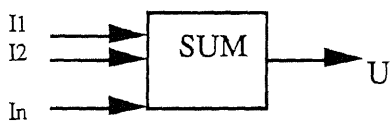
$U(t) = \Sigma In$, Sum of inputs.

Most blocks have an input summing function. However, sometimes it is desirable to have access to the summed input. In those cases this SUM block is used. The SUM block should have at least 2 inputs.

16) TIMe Function Block

TIM   U
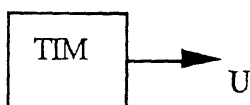
The output of the TIM block is the present time base of the simulation as specified in the "TIMING" dialog associated with model entry or the "CT" command. TIM gives access to the present simulation time, to allow the

generation of time dependent functions, such as SIN(t), etc. TIM is an input function. It has no inputs and no parameters.

APPENDIX B

This section shows the different volumes (Figures 24 - 35), pressures (Figures 36 - 47), and flows (Figures 48 - 59) for values of hemodynamic parameters given in Table 2.
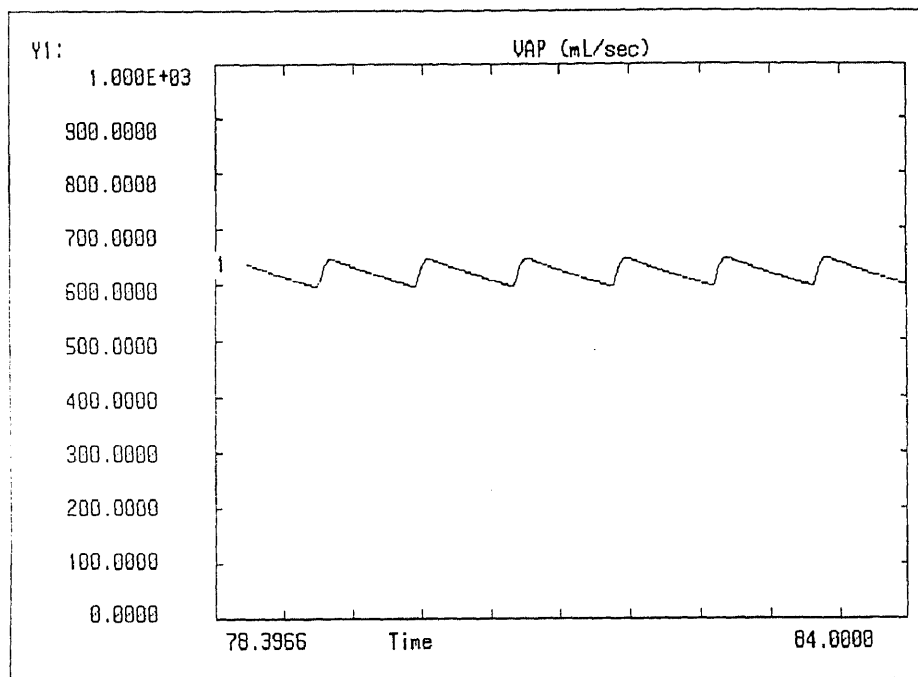
Figure 24 Volume in Pulmonary Arterial System vs Time for Values of
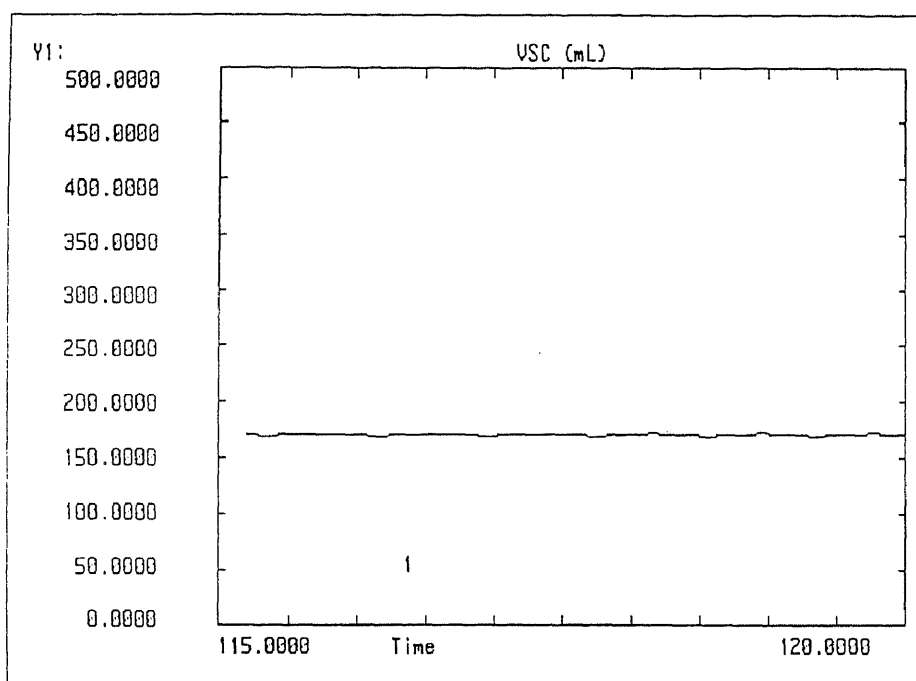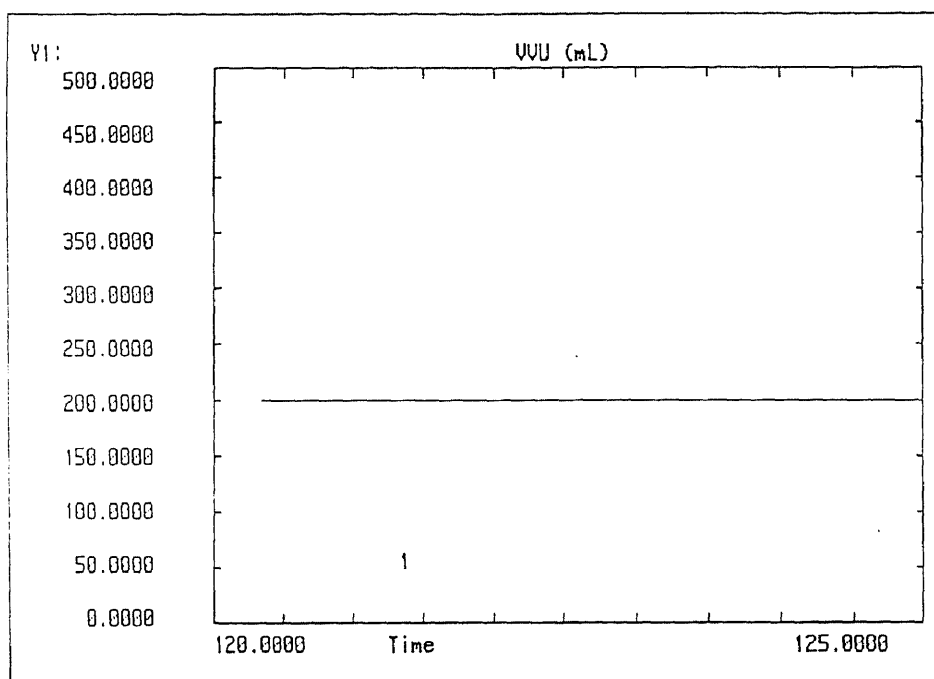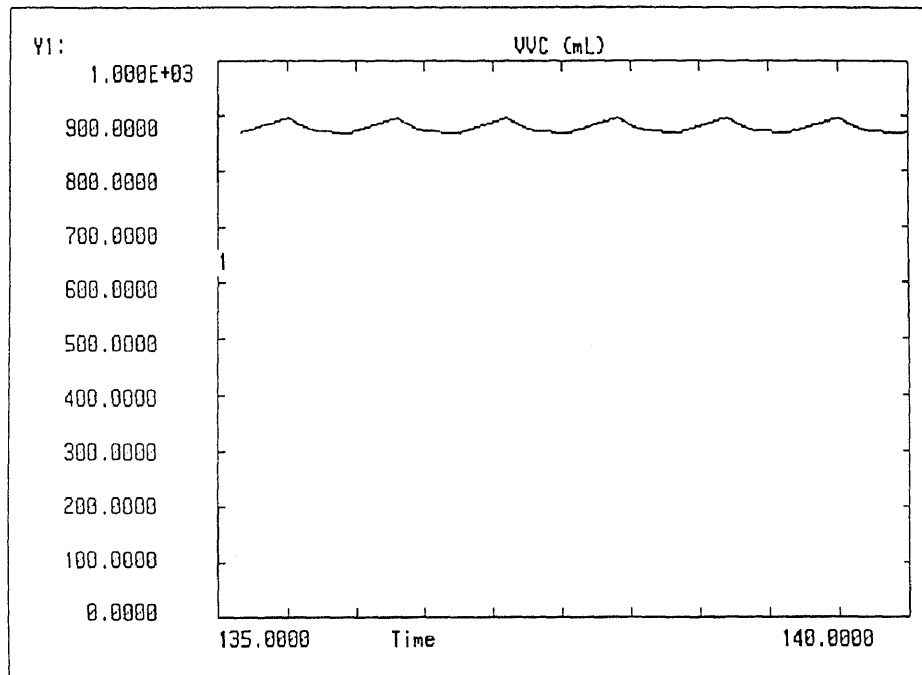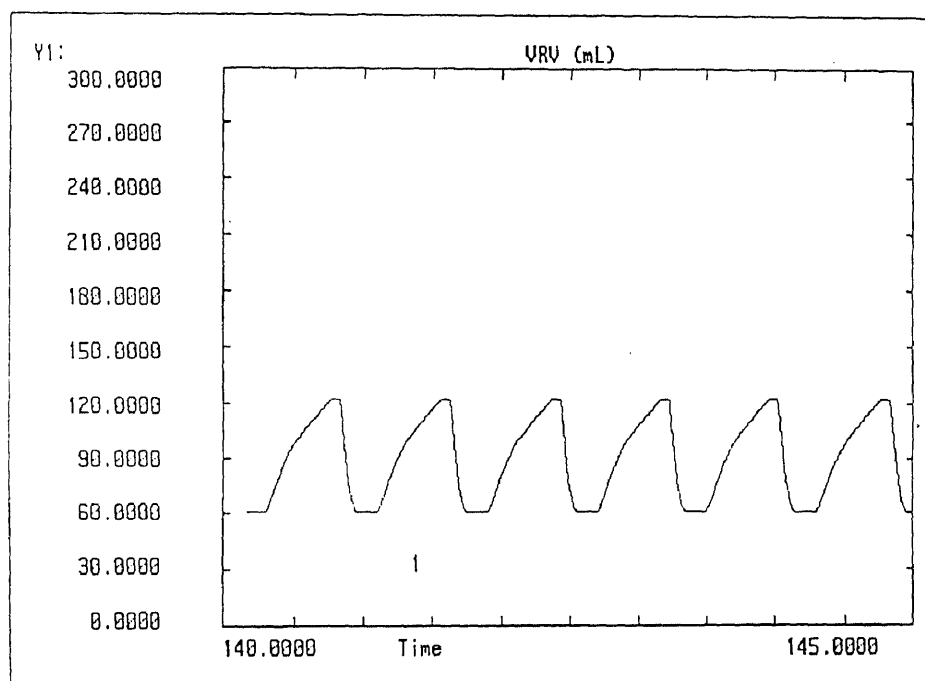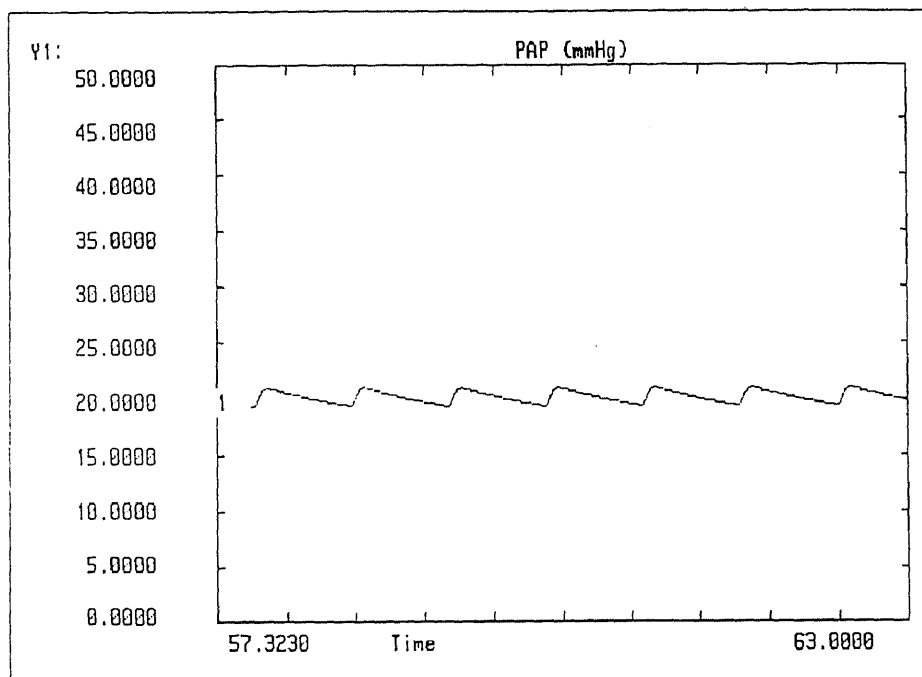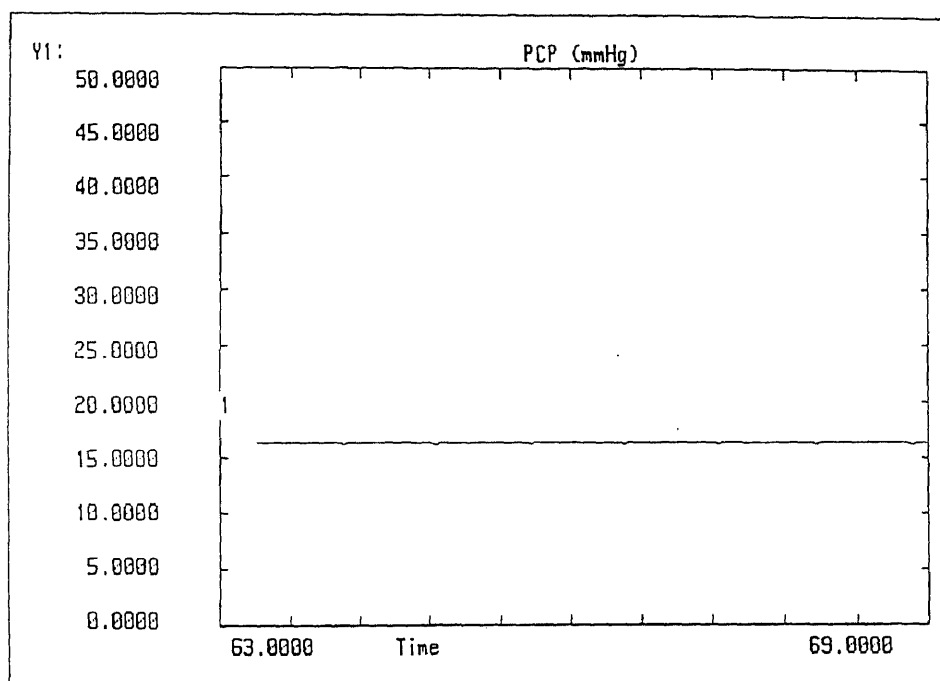Hemodynamic Parameters given in Table 2
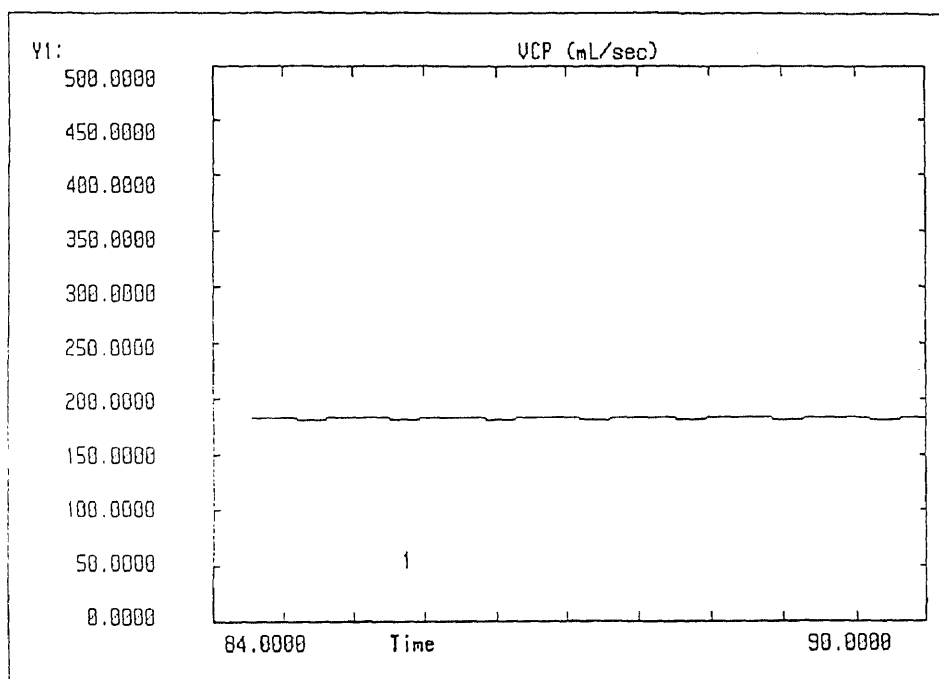
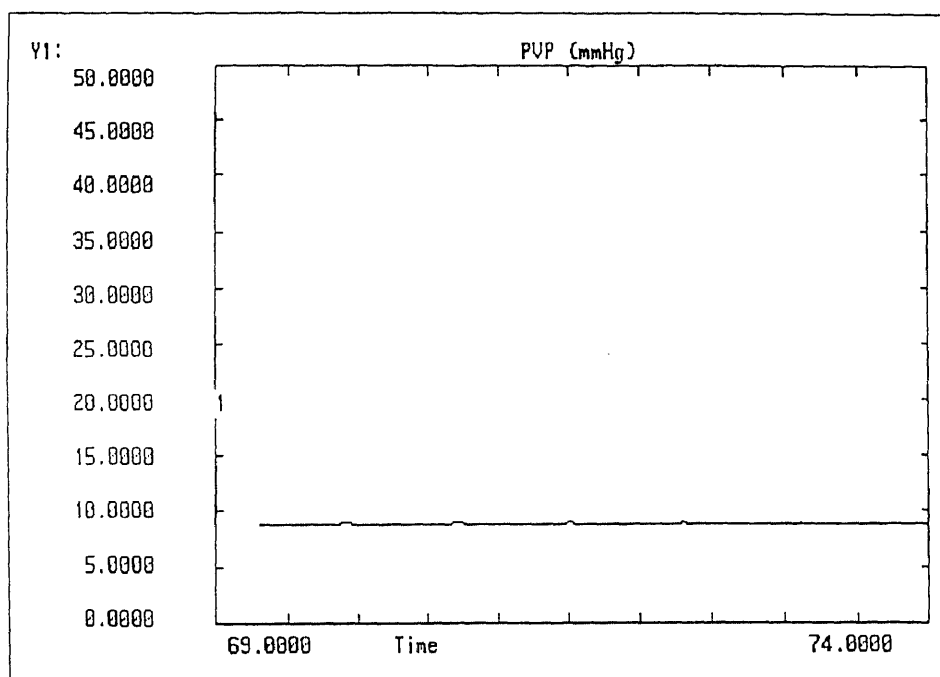**Figure 25** Volume in Pulmonary Capillary System vs Time for Values of Hemodynamic Parameters given in Table 2
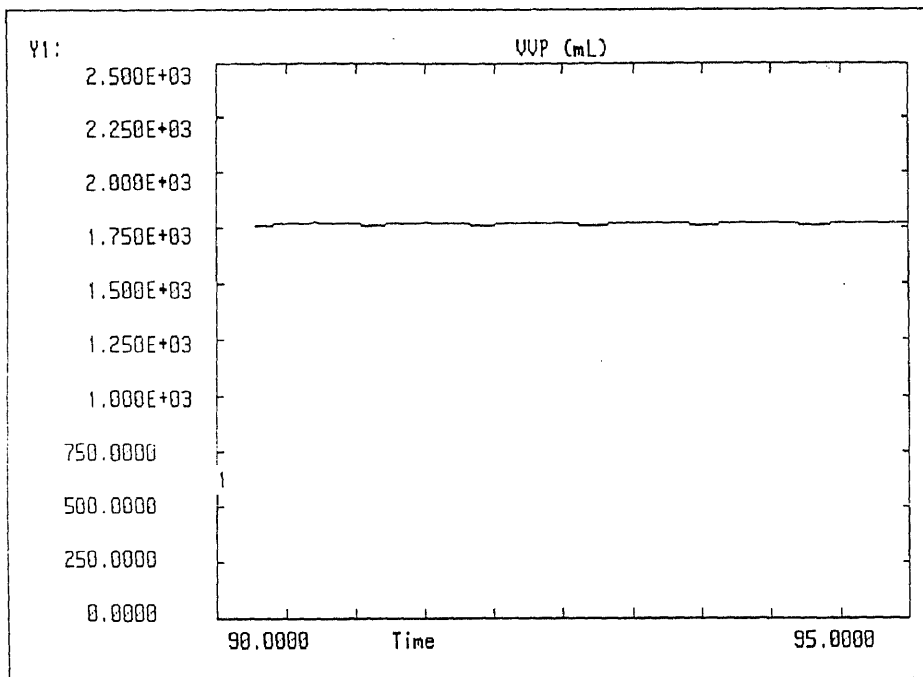
Figure 26 Volume in Pulmonary Venous System vs Time for Values of
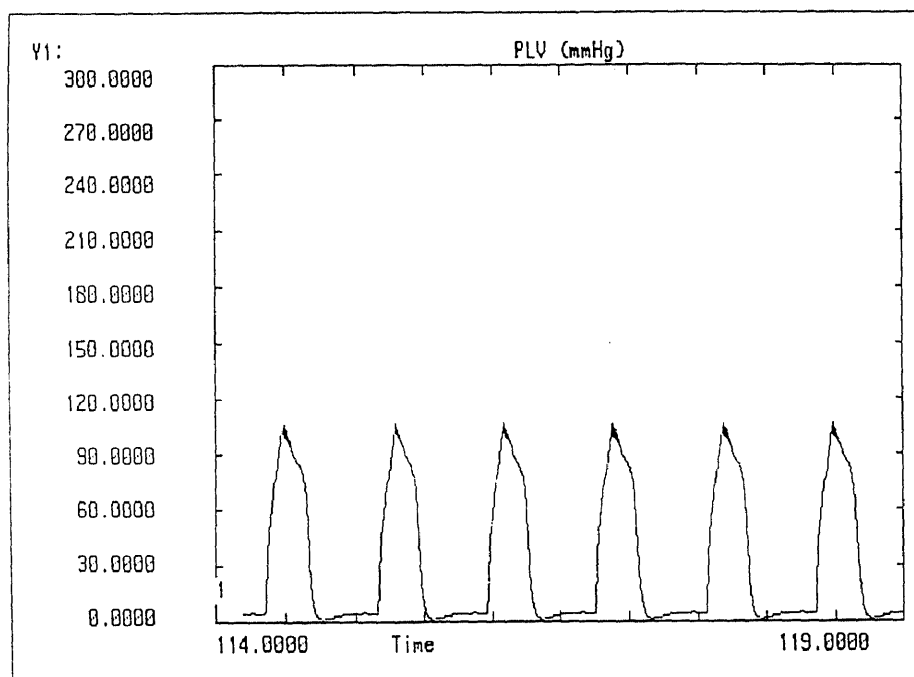Hemodynamic Parameters given in Table 2
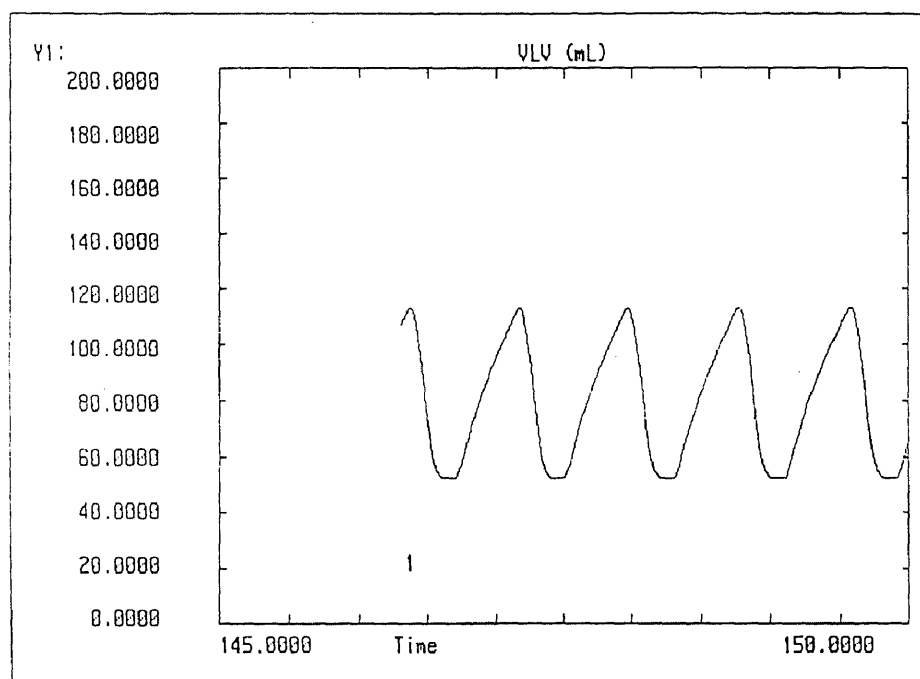
Figure 27 Volume in Left Ventricle vs Time for Values of Hemodynamic
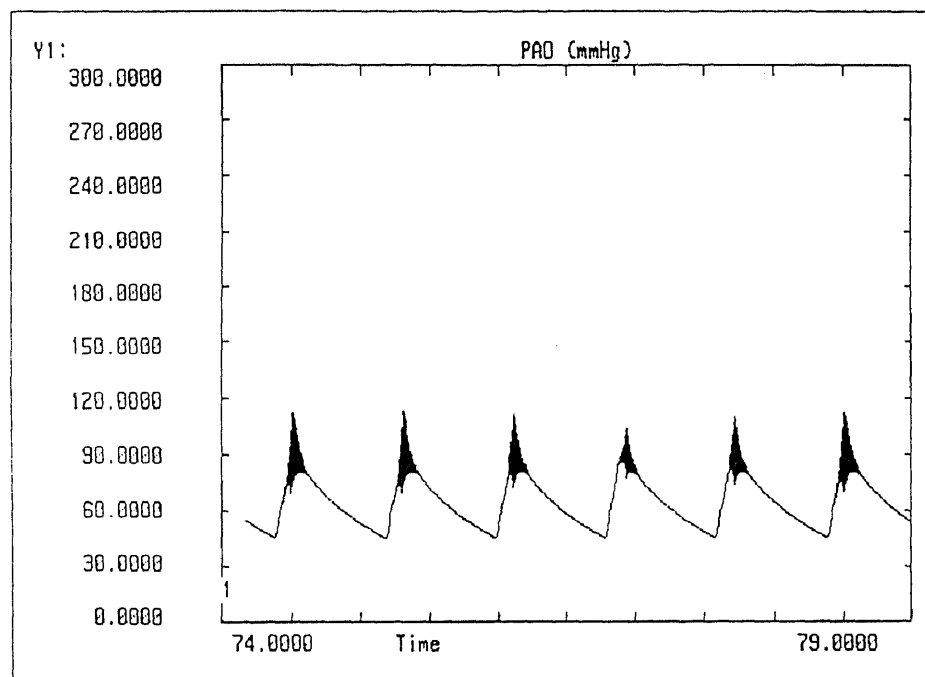Parameters given in Table 2
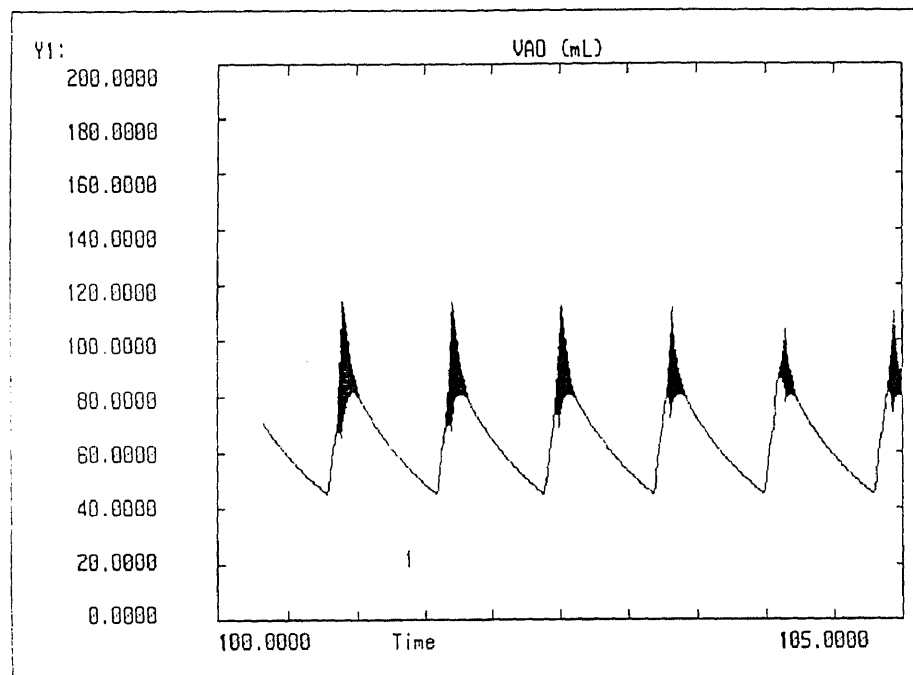
Figure 28 Volume in Aorta vs Time for Values of Hemodynamic
Parameters given in Table 2
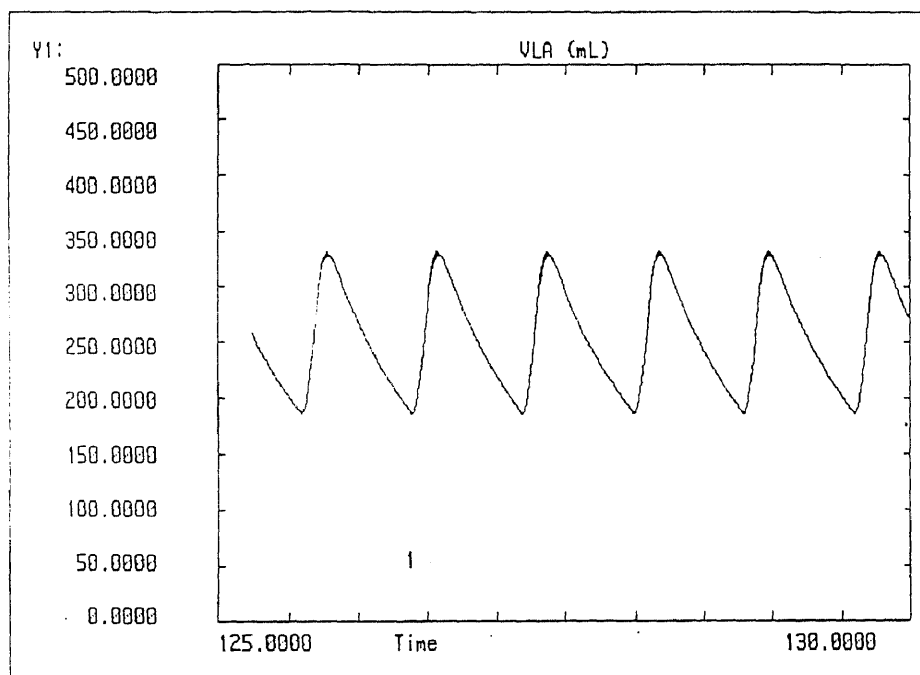
Figure 29 Volume in Large Arteries vs Time for Values of Hemodynamic
Parameters given in Table 2
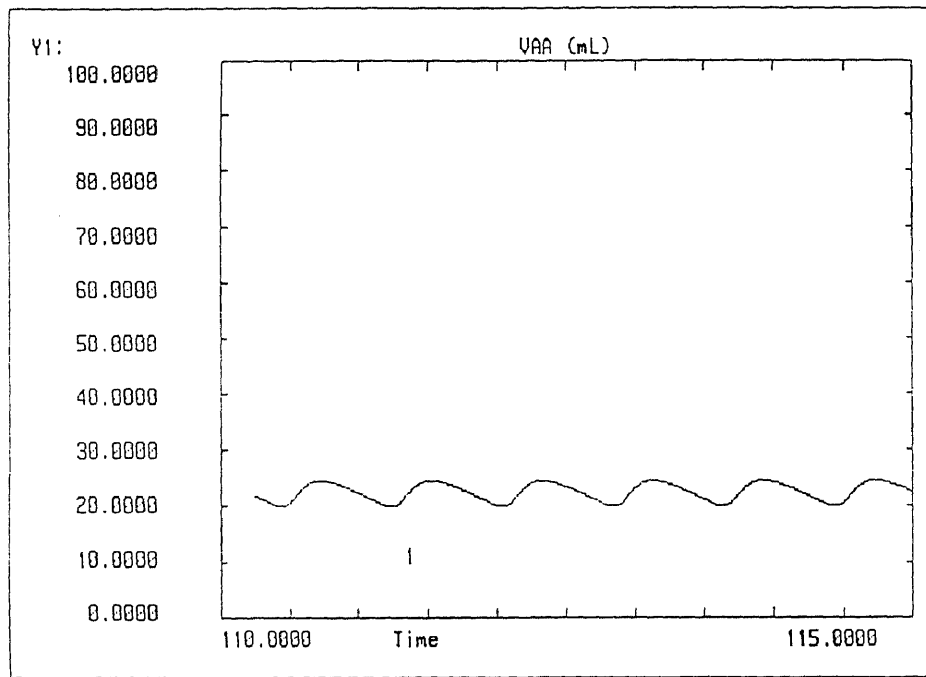
Figure 30 Volume in Arterioles vs Time for Values of Hemodynamic
Parameters given in Table 2

Figure 31 Volume in Systemic Capillaries vs Time for Values of
Hemodynamic Parameters given in Table 2

Figure 32 Volume in Venules vs Time for Values of Hemodynamic
    Parameters given in Table 2
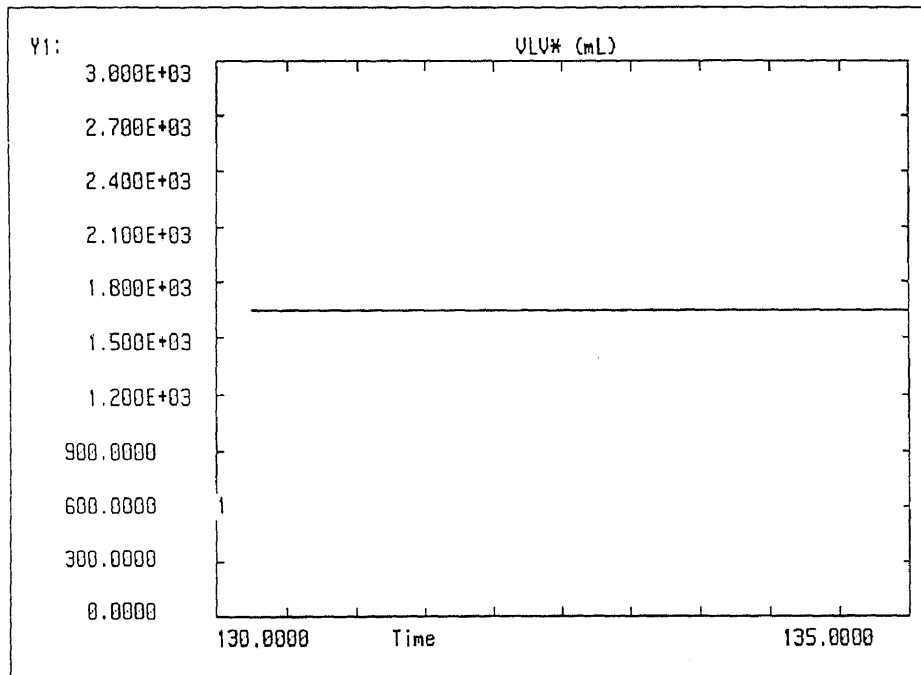
Figure 33 Volume in Large Veins vs Time for Values of Hemodynamic
Parameters given in Table 2

Figure 34 Volume in Vena Cava vs Time for Values of Hemodynamic
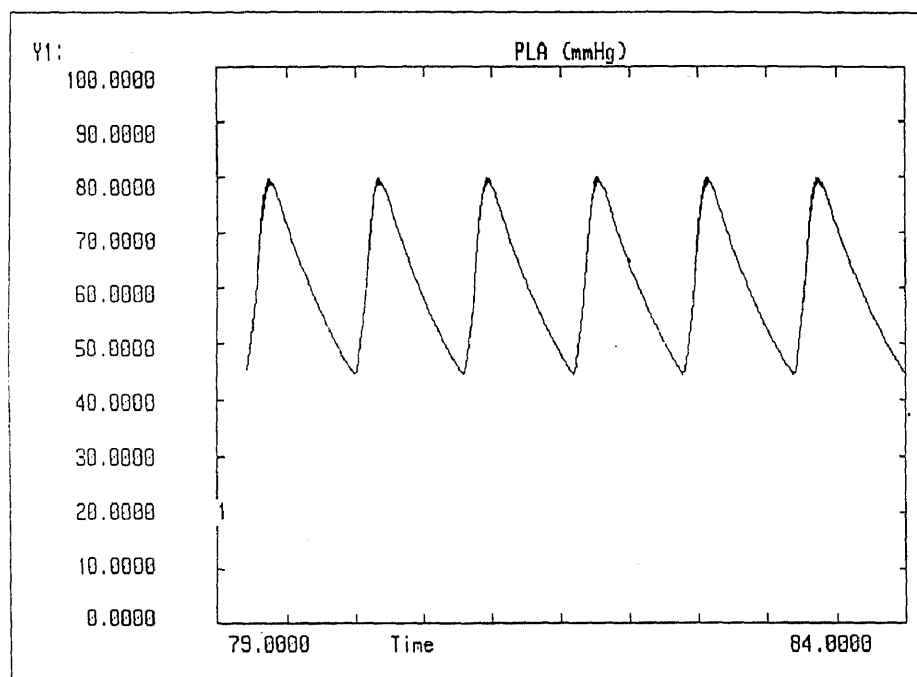Parameters given in Table 2

Figure 35 Volume in Right Ventricle vs Time for Values of Hemodynamic
Parameters given in Table 2
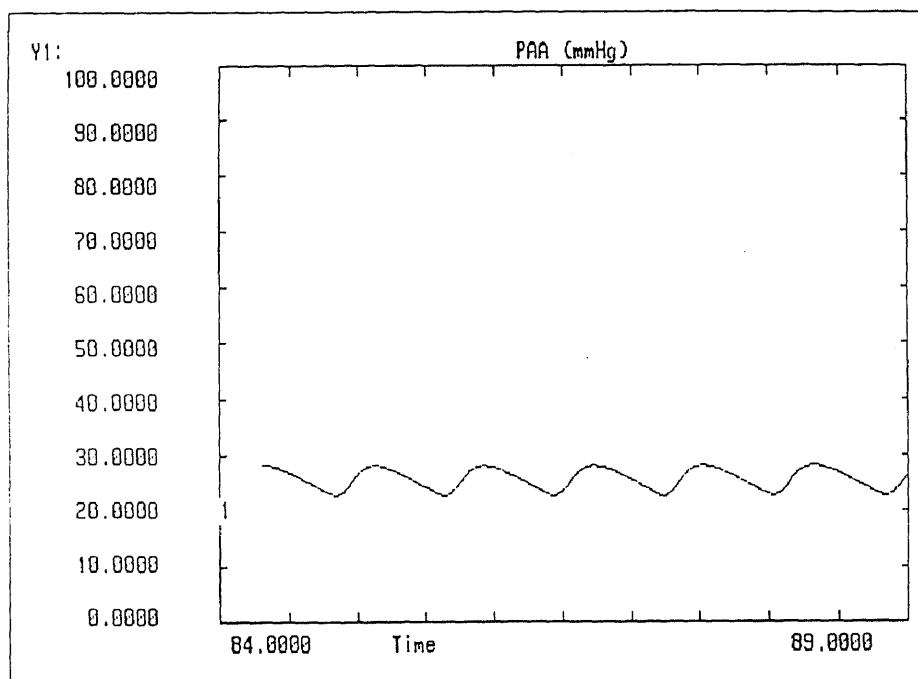
Figure 36 Pressure in Pulmonary Arterial System vs Time for Values of Hemodynamic Parameters given in Table 2

Figure 37 Pressure in Pulmonary Capillary System vs Time for Values of
Hemodynamic Parameters given in Table 2

Figure 38 Pressure in Pulmonary Venous System vs Time for Values of
Hemodynamic Parameters given in Table 2

Figure 39 Pressure in Left Ventricle vs Time for Values of Hemodynamic
Parameters given in Table 2

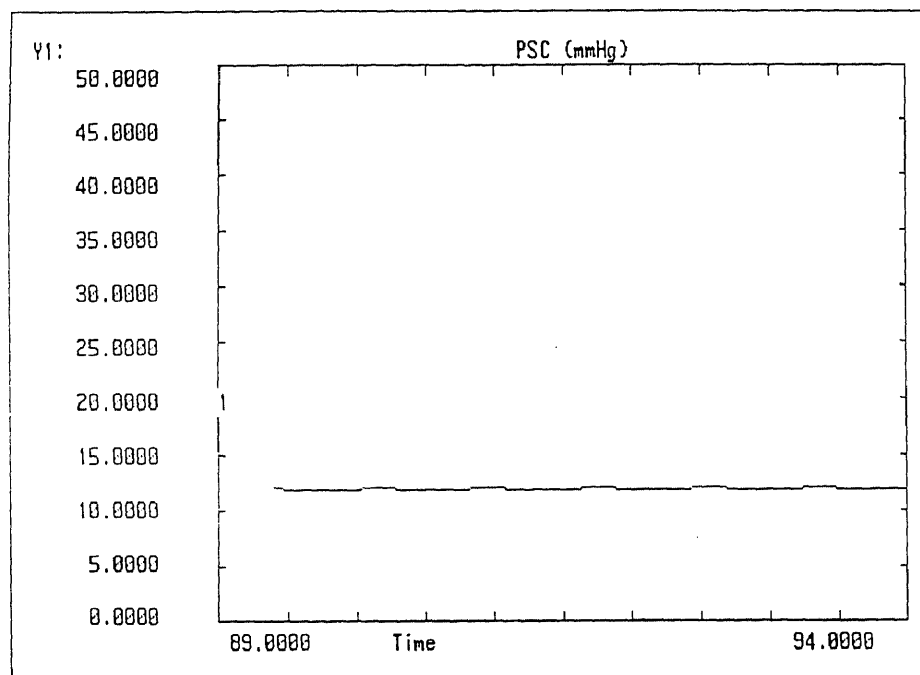Figure 40 Pressure in Aorta vs Time for Values of Hemodynamic
Parameters given in Table 2

Figure **41** Pressure in Large Arteries vs Time for Values of Hemodynamic
    Parameters given in Table 2

Figure 42 Pressure in Arterioles vs Time for Values of Hemodynamic
Parameters given in Table 2

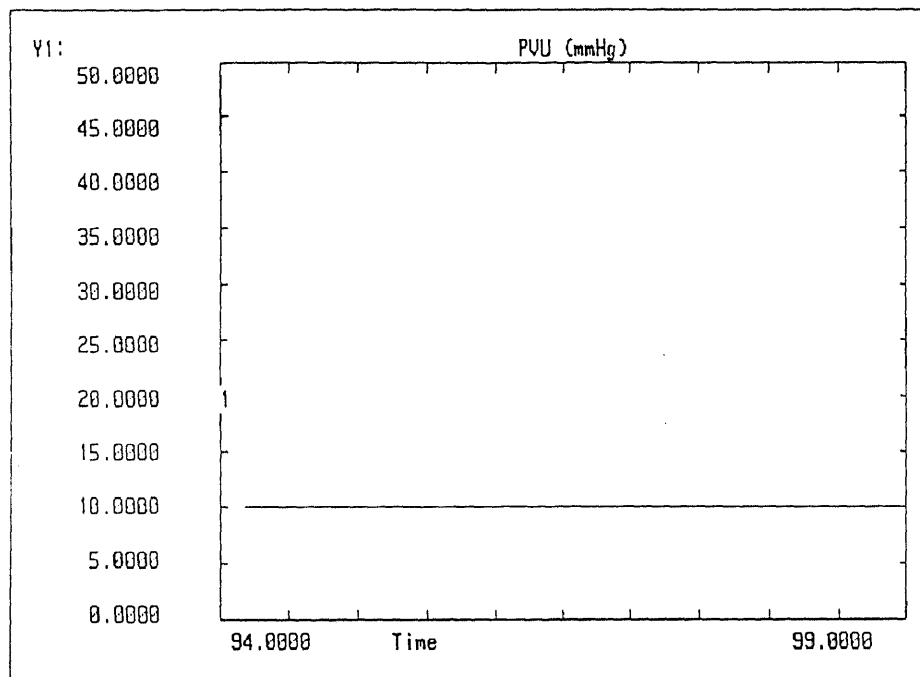**Figure 43** Pressure in Systemic Capillaries vs Time for Values of Hemodynamic Parameters given in Table 2

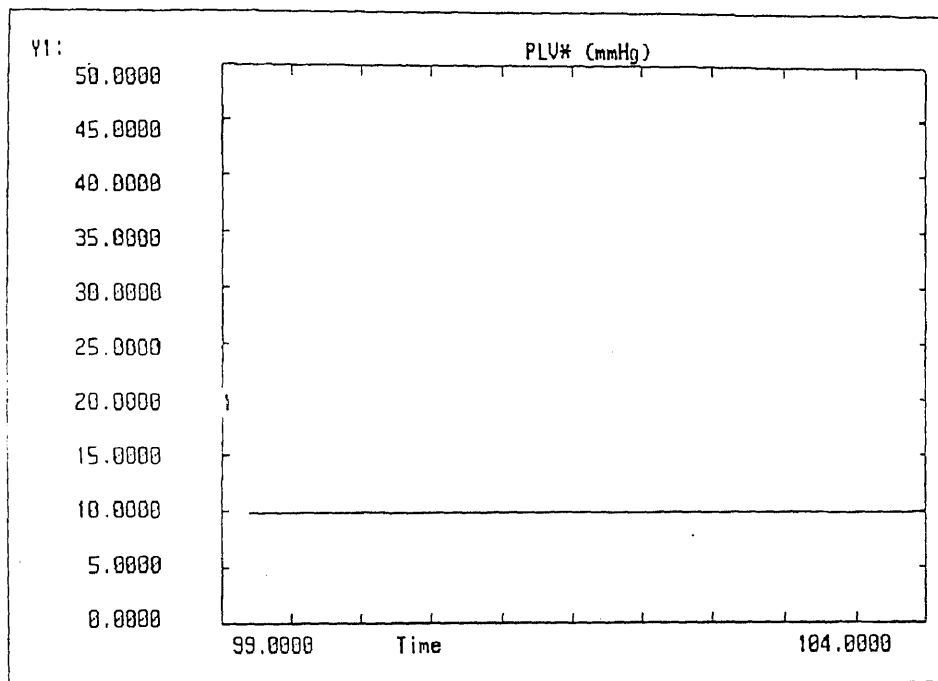**Figure 44** Pressure in Venules vs Time for Values of Hemodynamic Parameters given in Table 2

Figure 45 Pressure in Large Veins vs Time for Values of Hemodynamic
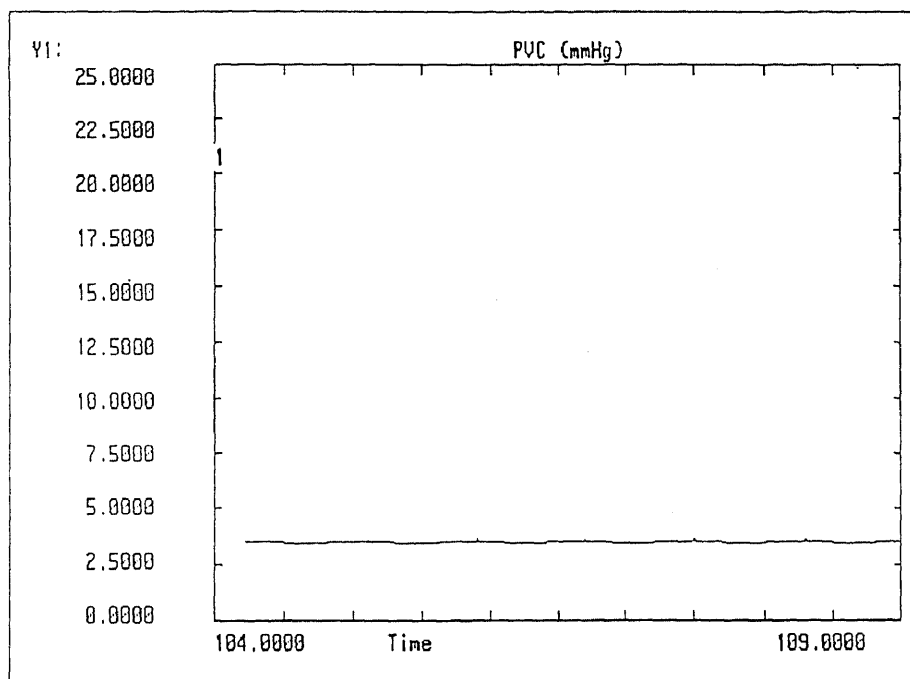Parameters given in Table 2

Figure 46 Pressure in Vena Cava vs Time for Values of Hemodynamic
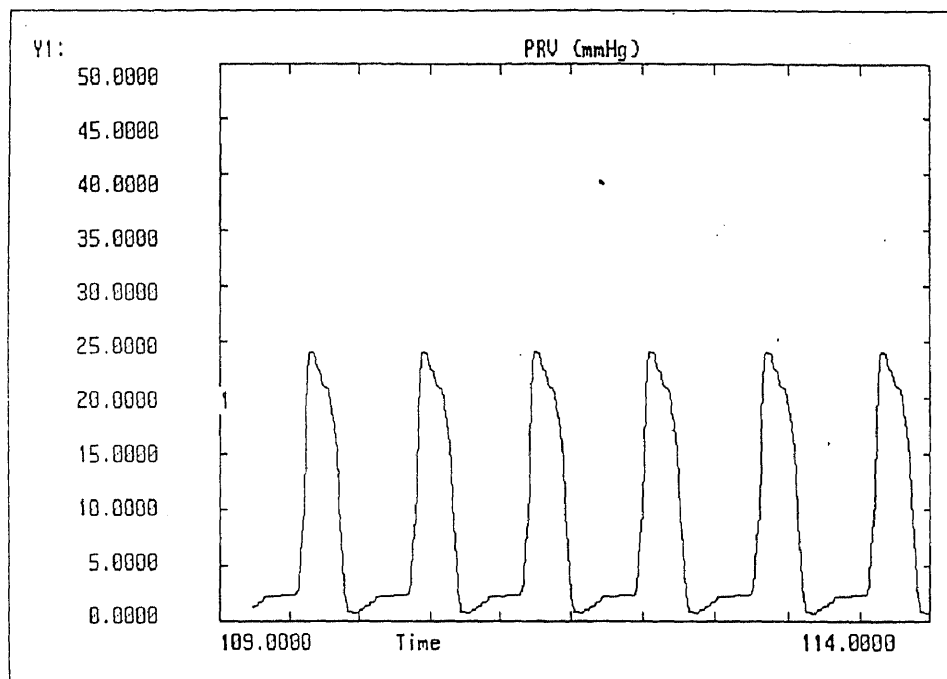Parameters given in Table 2

Figure 47 Pressure in Right Ventricle vs Time for Values of
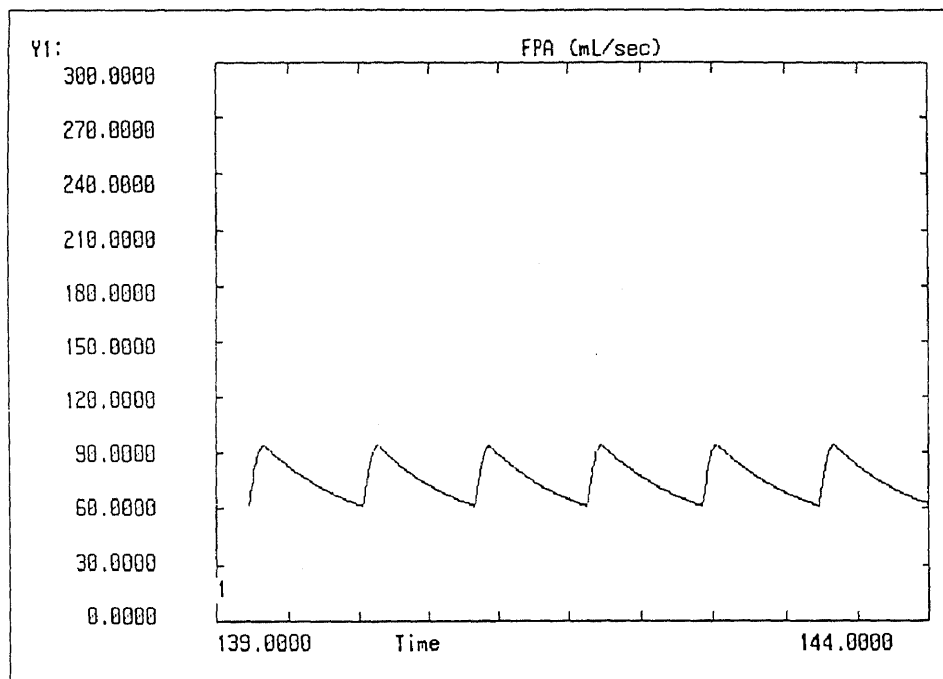Hemodynamic Parameters given in Table 2

Figure 48 Flow in Pulmonary Capillary System vs Time for Values of
Hemodynamic Parameters given in Table 2

Y1:   FPS (mL/sec)
  200.0000
  180.0000
  160.0000
  140.0000
  120.0000
  100.0000
   80.0000
   60.0000
   40.0000
   20.0000
    0.0000
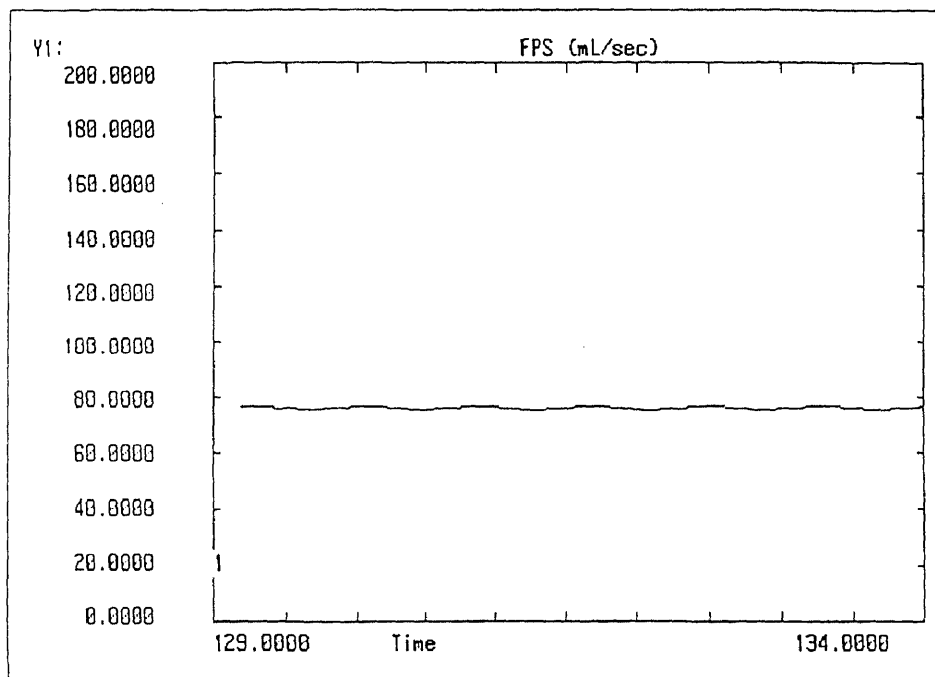   129.0000   Time   134.0000

Figure 49 Flow in Pulmonary Venous System vs Time for Values of
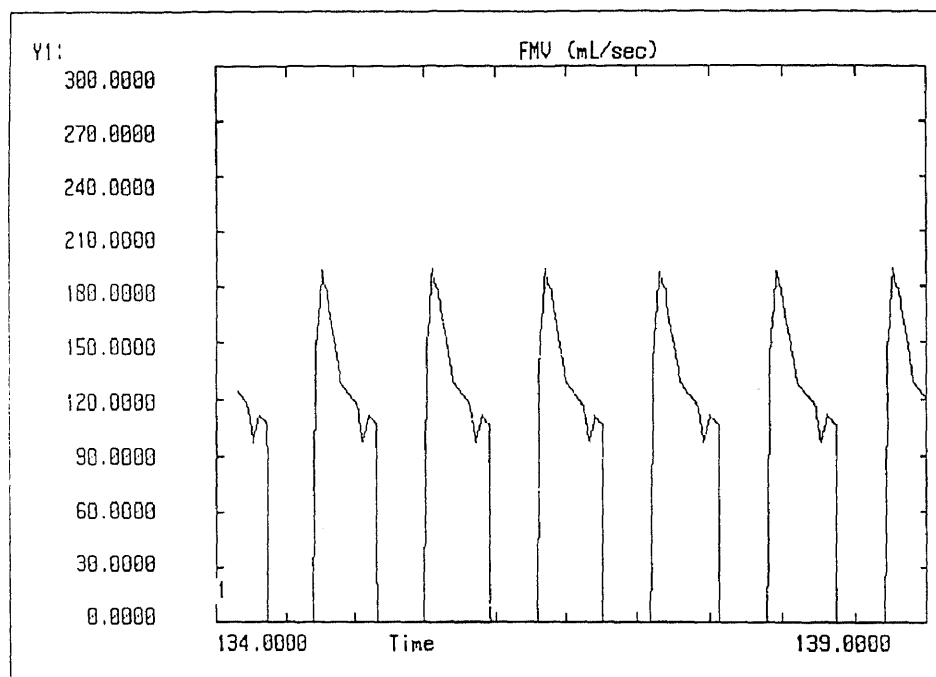Hemodynamic Parameters given in Table 2

Figure 50 Flow in Left Ventricle vs Time for Values of Hemodynamic
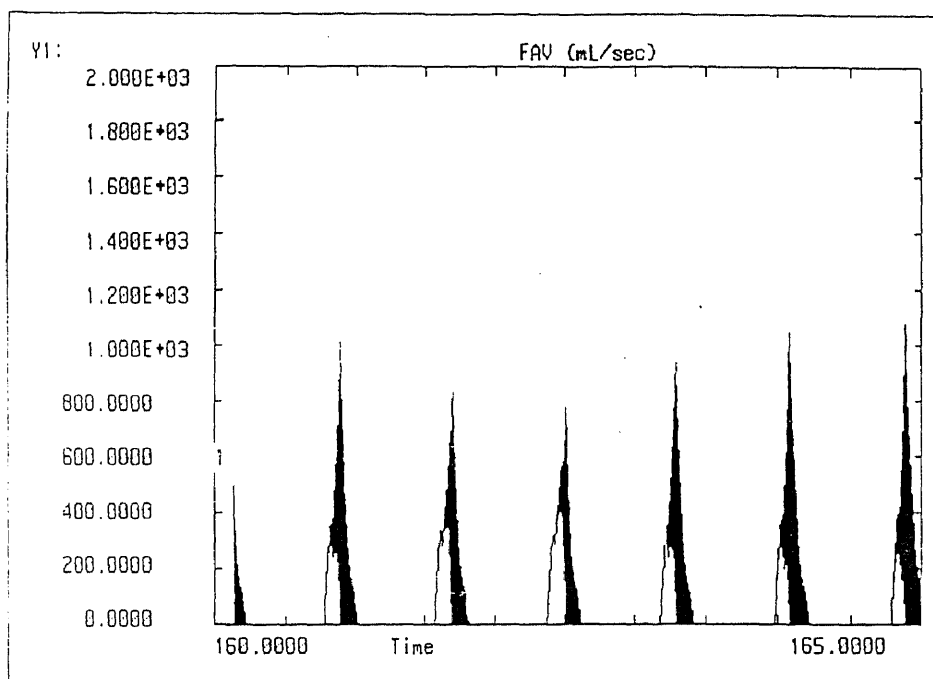Parameters given in Table 2

Figure 51 Flow in Aorta vs Time for Values of Hemodynamic Parameters
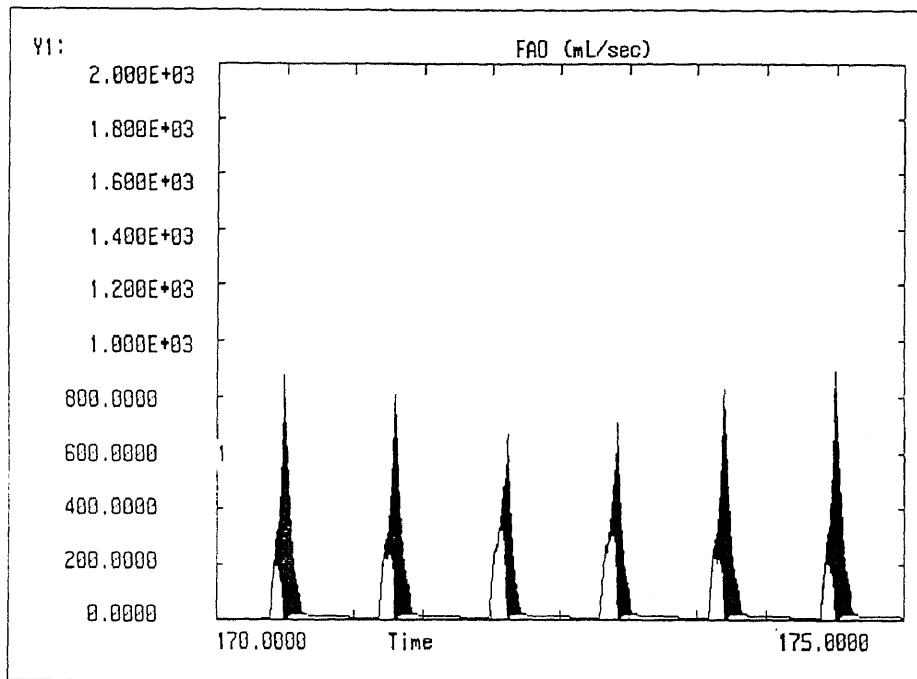given in Table 2

Figure 52 Flow in Large Arteries vs Time for Values of Hemodynamic Parameters given in Table 2
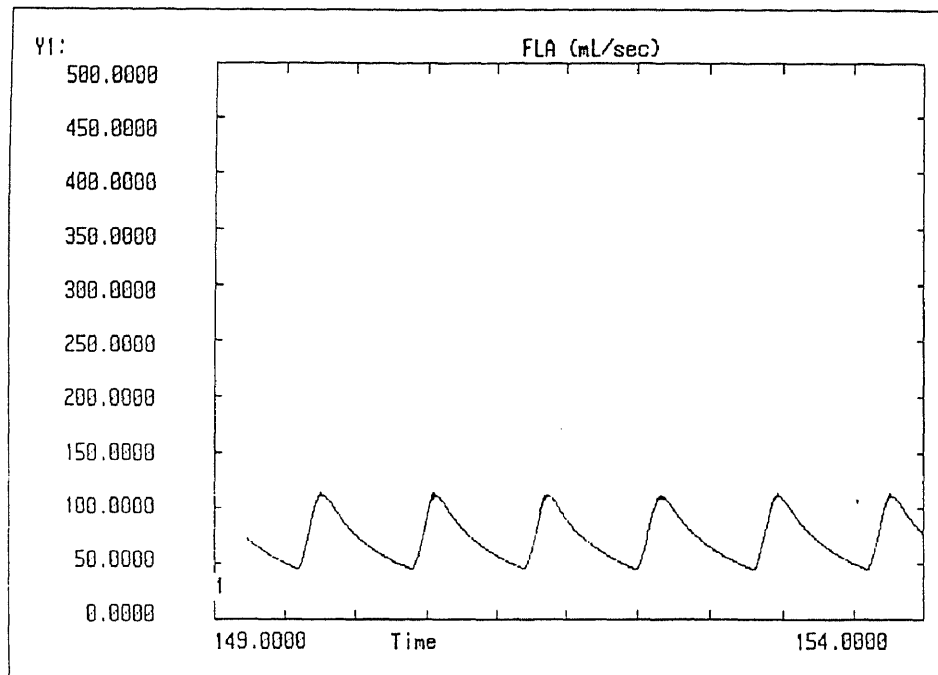
Figure 53 Flow in Arterioles vs Time for Values of Hemodynamic Parameters given in Table 2

Figure 54 Flow in Systemic Capillaries vs Time for Values of
Hemodynamic Parameters given in Table 2

Figure 55 Flow in Venules vs Time for Values of Hemodynamic
Parameters given in Table 2

Y1:
FV2 (mL/sec)

100.0000
90.0000
80.0000
70.0000
60.0000
50.0000
40.0000
30.0000
20.0000
10.0000
0.0000

100.0000   Time   105.0000

Figure 56 Flow in Large Veins vs Time for Values of Hemodynamic
Parameters given in Table 2

Figure 57 Flow in Vena Cava vs Time for Values of Hemodynamic
Parameters given in Table 2

Figure 58 Flow in Right Ventricle vs Time for Values of Hemodynamic
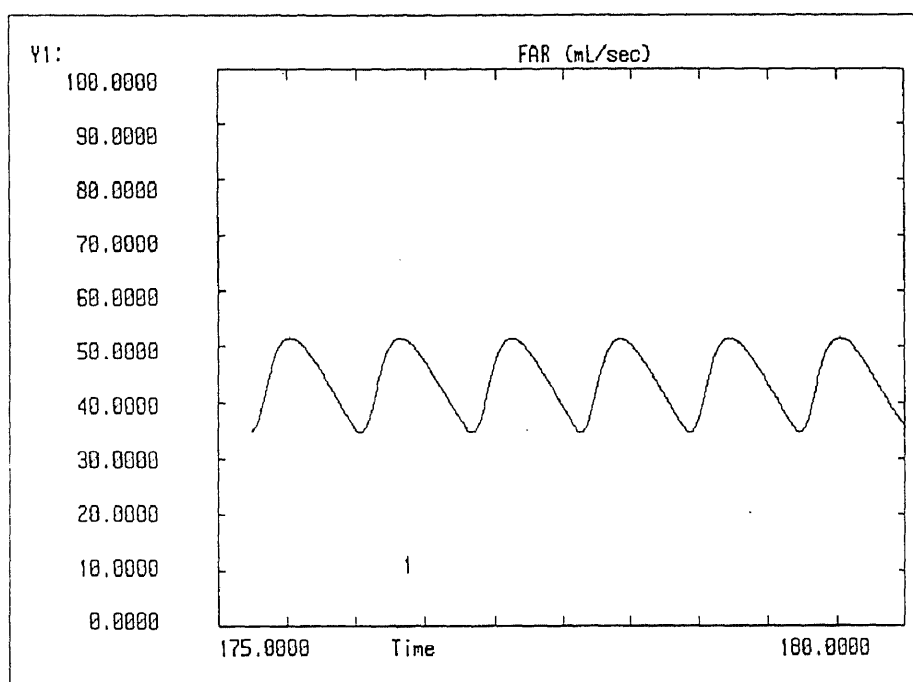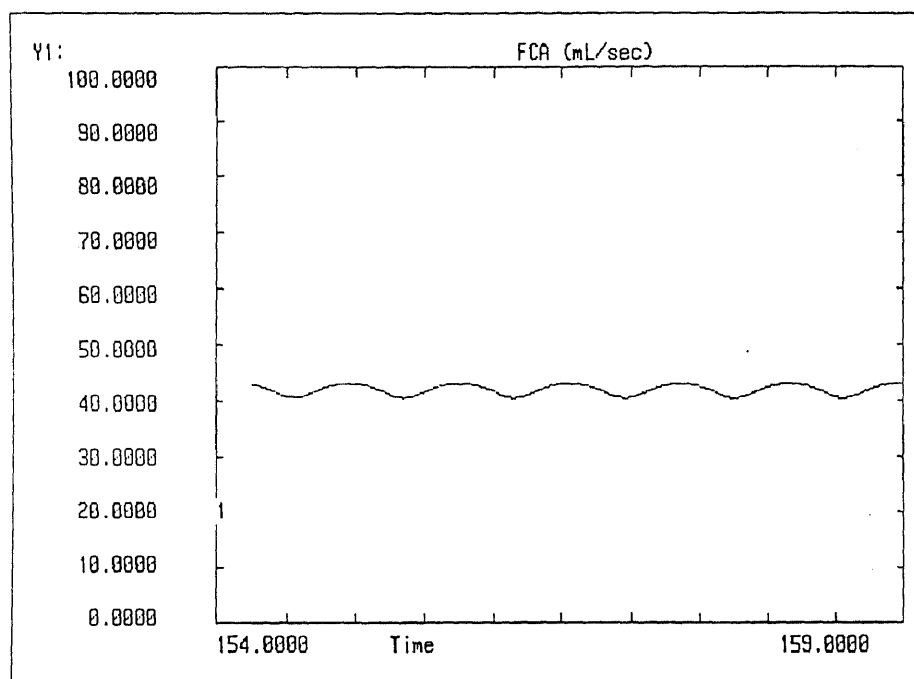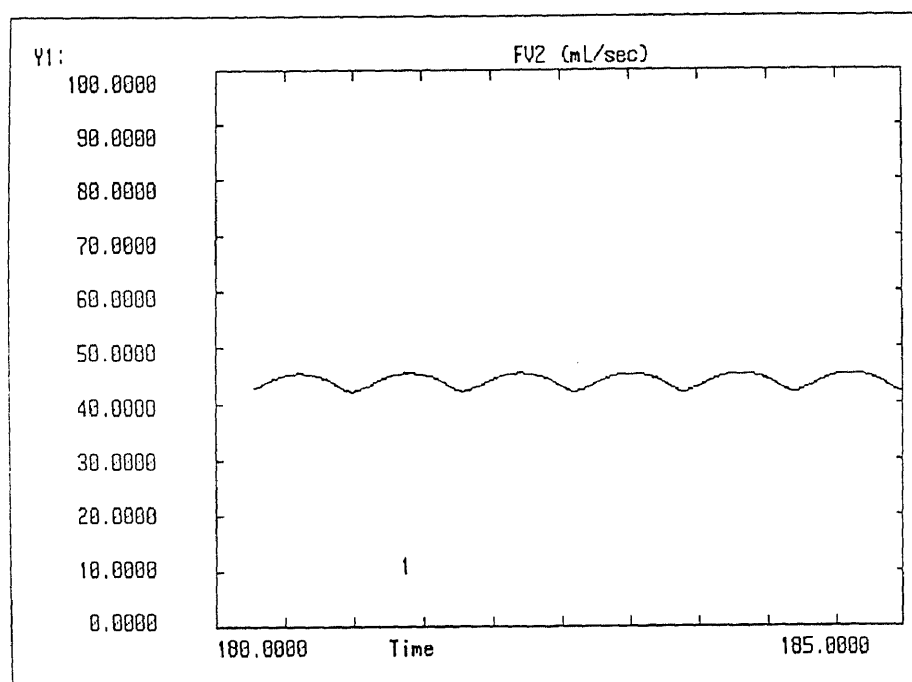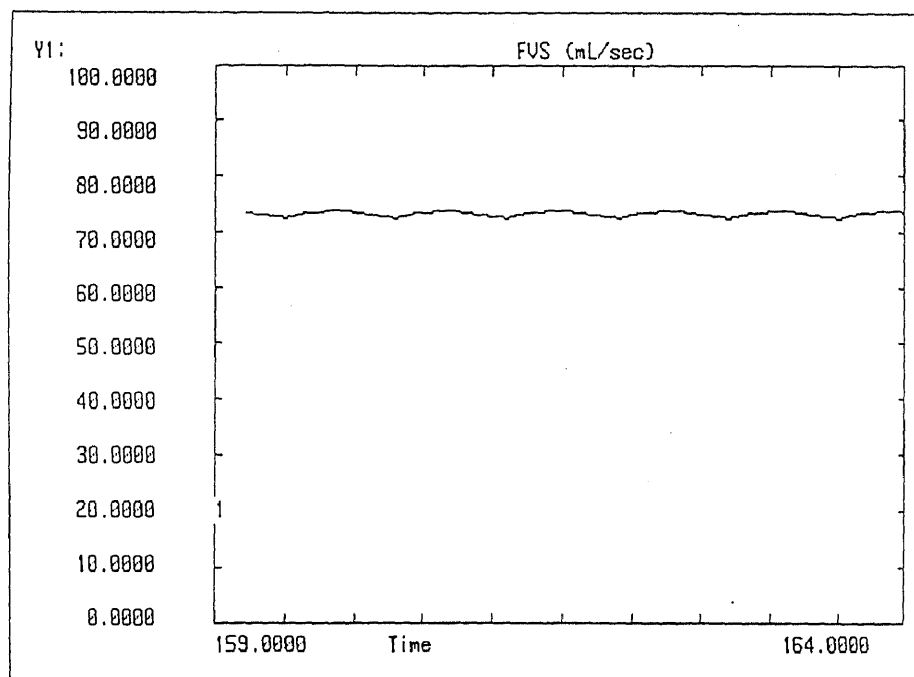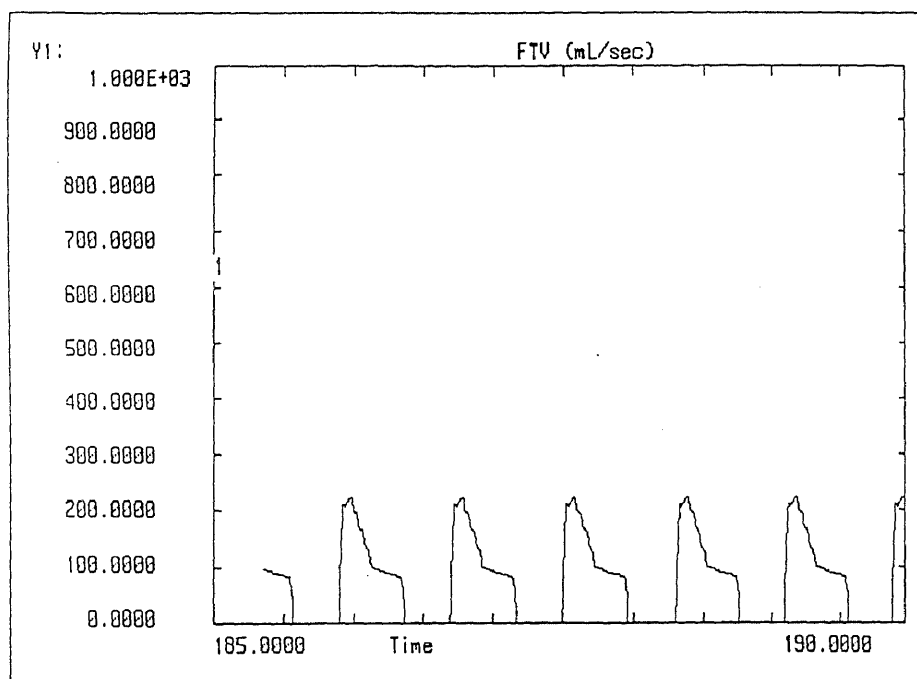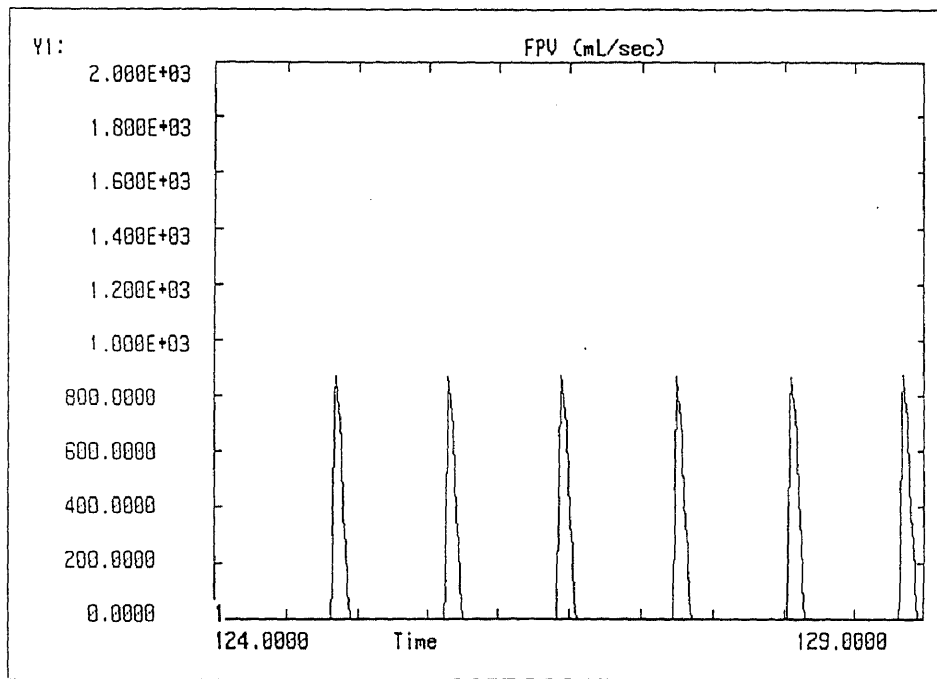Parameters given in Table 2

Figure 59 Flow in Pulmonary Arterial System vs Time for Values of Hemodynamic Parameters given in Table 2

BIBLIOGRAPHY

[1]   Baller, D., H. J. Bretschneider, and G. Hellige. "Validity of Myocardial
       Oxygen Consumption Parameters." *Clinical Cardiology.* 2 (1979):
       317-327.

[2]   Boyle III, Joseph. "Microcomputer Analysis of Oxygen Transport and
       Tissue PO_2 in Shock." *Mathematical Modelling.* 7 (1986): 1635-
       1649.

[3]   Cooney, David O. "Biomedical Engineering Principles: An
       Introduction to Fluid, Heat, and Mass Transport Processes."
       Marcel and Dekker Inc., New York and Bassel. 2 (1976).

[4]   Elzinga, G., and N. Westerhof. "Pressure-Volume Relations in Isolated
       Cat Trabecula." *Circulation Research.* 49 (1981): 388-394.

[5]   Evans, C. L., and Y. Matsuoka. "The Effect of Various Mechanical
       Conditions on the Gaseous Metabolism and Efficiency of the
       Mammalian Heart." *Journal of Physiology* (London). 49 (1915):
       378-405.

[6]   Frank, O. "Die Grundform Des Arteiellen Pulses." *Z Biol.* 36 (1895):
       483-526.

[7]   Green, J. H., and P. F. Heffron. "Studies Upon the Relationship between
       Baroreceptor and Sympathetic Activity." *Q. J. Experimental
       Physiology.* 53 (1968): 23-32.

[8]   Greenway, C. V. "Mechanisms and Quantitative Assessment of Drug
       Effects on Cardiac Output with a New Model of the Circulation."
       Pharmacological Reviews.. 33 (1982): 213-251.

[9]   Guyton, A. C, T. G Coleman, and H. J. Granger. "Circulation : Overall
       Regulation." *Annual Rev. Physiology.* 34 (1972): 13-46.

[10]   Guyton, A. C, C. E. Jones, and T. G. Coleman. "Circulatory Physiology :
       Cardiac Output and its Regulation." *Circulatory Physiology. 2nd
       ed.,* W. B Saunders, Philadelphia. (1973): 556

[11]   Hoeft, A., H. Sonntag, H. Stephan, and D. Kettler. "Validation of
       Myocardial Oxygen Demand Indices in Patients Awake and
       During Anesthesia." *Anesthesiology.* 75 (1991): 419-456.

[12]   Korner, P. I. "Central and Peripheral Resetting of the Baroreceptor
       System." *Clinical and Experimental Pharmacological Physiology.*
       2 (1975): 171-178.

104

[13] Levy, M. N. "The Cardiac and Vascular Factors that Determine Systemic Blood Flow." *Circulation Research.* 44 (1979): 739-746.

[14] Madwed, J. B. "Dynamic Analysis of Arterial Blood Pressure and Heart Rate During Baseline Conditions and Hemorrhage in the Conscious Dog." *(PhD Thesis). Boston, MA,* (1987) Harvard Medical School, Department of Physiology.

[15] Madwed, J. B., P. Albrecht, G. R. Mark, and R. J. Cohen. "Low Frequency Oscillations in Arterial Pressure and Heart Rate." *American Journal of Physiology.* 256 (1989): H1573-H1579.

[16] McLeod, John P. E. "PHYSBE - Model of the Heart." *TUTSIM Simulation for Design and Analysis,* TUTSIM Products, CA (1991).

[17] Mitchell, J. H, A. G. Wallace, and N. S. Skinner. "Intrinsic Effects of Heart Rate on Left Ventricular Performance." *American Journal of Physiology.* 205 (1963): 41-48.

[18] Monroe, H. G., and G. N. French. "Left Ventricular Pressure-Volume Relationships and Myocardial Oxygen Consumption in the Isolated Heart." *Circulation Research.* 9 (1961): 362-374.

[19] Polosa, C. "Rhythms in the Activity of the Autonomous Nervous System: Their Role in the Generation of Systemic Arterial Pressure Waves. "*Mechanisms of blood pressure waves,* edited by K. Miyakawa, H. P. Koepchen, and C. Polosa , Tokyo: Japan Science Society Press. (1984): 27-41.

[20] Rhode, E. "Uber Den Einflu Beta Der Mechanishen Bedingungen Auf Die Tatigkeit und den Sauerstoffverbrauch des Warmbluterherzens." *Archiv. fur experimentelle Pathologie und Pharmakologie.* 68 (1915): 401-434.

[21] Rooke, G. A., and E. O. Feigel. "Work as a Correlate of Canine Left Ventricular Oxygen Consumption, and the Problem of Catecholamine Wasting." *Circulation Research.* 50 (1982): 273-286.

[22] Rothe, C. F. "A Computer Model of the Cardiovascular System for Effective Learning." *Physiologist.* 23 (1981): 49-52.

[23] Schwid, Howard A., C. W. Buffington, and P. Strum. "Computer Simulation of the Hemodynamic Determinants of Myocardial Oxygen Supply and Demand." *Journal of Cardiothoracic Anesthesia.* 4 (1990): 5-18.

[25]   Siegel, John H. "Through a Glass Darkly: the Lung as a Window to
       Monitor Oxygen Consumption, Energy Metabolism, and Severity
       of Critical Illness." *Clin. Chem.* 3618 (1990): 1585-1593.

[26]   Siegel, J. H, S. E. Linberg, and C. E. Wiles. "Therapy of Low-Flow Shock
       States." In : Siegel J. H. ed. *Trauma : emergency surgery and critical
       care.* New York: Churchill Livingstone. (1987): 201-284.

[27]   Suga, H. "Total Mechanical Energy of a Ventricle Model and Cardiac
       Oxygen Consumption." *American Journal of Physiology.* 236
       (1979): 498-505.

[28]   Suga, H., R. Hisano, Y. Goto, O. Yamada, and Y. Igarashi. "Effect of
       Positive Inotropic Agents on the Relation between Oxygen
       Consumption and Systolic Pressure-Volume Area in Canine Left
       Ventricle." *Circulation Research.* 53 (1983): 306-318.

[29]   Suga, H. and K. Sagawa. "Instantaneous Pressure-Volume
       Relationships and Their ratio in the Excised, Supported Canine
       Left Ventricle." *Circulation Research.* 35 (1974): 117-126.

[30]   Suga, H., K. Sagawa, and L. Demer. "Determinants of Instantaneous
       Pressure in Canine Left Ventricle: Time and volume
       Specification." *Circulation Research.* 46 (1980): 256-263.

[31]   Sagawa, H., K. Sagawa, and A. A. Shoukas."Load Independence of the
       Instantaneous Pressure-Volume Ratio of the Canine Left
       Ventricle and Effects of Epinephrine and Heart Rate on the
       Ratio. "*Circulation Research.* 32 (1973): 314-322.

[32]   Starling, E. H., and M. B. Visscher. "The Regulation of the Energy
       Output of the Heart." *Journal of Physiology* (London). 62 (1927):
       243-261.

[33]   Sunagawa, K., and K. Sagawa. "Models of Ventricular Contraction
       Based on Time-Varying Elastance." *CRC Critical Review
       Biomedical Engineering.* 7 (1982): 193-228.

[34]   Taylor, R. R. "Active Length-Tension Relations Compared in
       Isometric, Afterloaded and Isotonic Contractions of Cat
       Papillary Muscle." *Circulation Research.* 26 (1970): 279-288.